

UNIVERSIDADE DE LISBOA
FACULDADE DE CIÊNCIAS
DEPARTAMENTO DE BIOLOGIA VEGETAL



**Ciências
ULisboa**

Epitranscriptomic deregulation in bladder cancer: Implications for tumour aggressiveness

Catarina Sofia Guimarães Teixeira

Mestrado em Biologia Molecular e Genética

Dissertação orientada por:
Professora Doutora Carmen de Lurdes Fonseca Jerónimo
Professora Doutora Margarida Gama Carvalho

2019

“Imagination is more important than knowledge. Knowledge is limited.

Imagination encircles the world.”

Albert Einstein



Cofinanciado por:



This study was funded by a grant of the Research Centre of Portuguese Oncology Institute of Porto

AGRADECIMENTOS

Um ano de trabalho, um ano de desafios, um ano de dúvidas e nunca de certezas, um ano de ciência! Aqui apresento o meu trabalho final, onde desde já agradeço a toda a gente que me ajudou e o tornou possível.

Em primeiro lugar gostaria de agradecer à minha orientadora, Professora Doutora Carmen Jerónimo por me ter aceite no maravilhoso Grupo de Epigenética e Biologia do Cancro, propondo-me um enorme desafio. Agradeço a sua disponibilidade para a resolução de todos os problemas científicos que surgiram, por todo o apoio e especialmente, por toda a paciência que teve comigo ao longo deste ano.

Em segundo lugar, ao Professor Doutor Rui Henrique que esteve sempre disponível para partilhar as suas ideias e para ajudar em tudo o que precisasse. Sem dúvida um grande contributo para o projeto.

Quero igualmente agradecer ao Diretor do Centro de Investigação deste instituto, Professor Doutor Manuel Teixeira, por ter permitido a minha presença e a de muitos outros estudantes, e me permitir concretizar este trabalho.

Uma palavra de agradecimento ao Engenheiro Luís Antunes pela sua disponibilidade e ajuda nos resultados estatísticos.

Expresso o meu agradecimento à Professora Doutora Margarida Gama Carvalho, minha orientadora interna, por me ter facilitado o intercâmbio entre a universidade de Lisboa e o IPO-Porto e me ter permitido desenvolver a minha dissertação.

Quero também deixar um enorme agradecimento, porque sem dúvida que foi uma pessoa essencial neste projeto, à Sara Monteiro Reis. Um verdadeiro apoio que me transmitiu imenso conhecimento, ajudou-me com todos os desafios neste percurso e aturou todos os meus dramas quando parecia que estava num beco sem saída. Um obrigado não chega!

Gostaria de deixar um agradecimento muito especial à Cláudia Lima que lutou muito para que a maldita coorte de bexiga em comum nos nossos projetos ficasse completa! Agradeço por me ter acompanhado de uma forma especial ao longo deste ano, por ter aturado as minhas manias, a minha maneira autoritária de falar e, especialmente, por ser a melhor pessoa que eu podia ter ao meu lado neste desafio.

Um gigante agradecimento a todas as pessoas que fazem parte da minha sala, companheiros de mestrado, Vera Constâncio, Rita Oliveira, Mariana Brütt e Gonçalo Pinho que sofreram da mesma dor que eu, as mais recentes mestres, Sandra Nunes, Catarina Macedo e Ana Lameirinhas, à aluna de doutoramento infiltrada, Daniela Barros, sem esquecer os mais recentes alunos de mestrado, Zé Pedro, Luísa e Filipa, e à Carina Maia, por nos mandar fazer os consentimentos nas alturas mais inoportunas. Eles que ouviram as minhas histórias diárias, sentiram a minha dor com as imunohistoquímica e *Western blot*, aturarem a personagem que é a “Teixas” e melhor de tudo, fizeram deste magnífico ano no Porto, o melhor que eu podia desejar. Uma nota particular para a Daniela Barros e Ana Lameirinhas porque de facto foram incansáveis na reta final e a ajuda delas foi preciosa!

Quero também agradecer às mais velhas, Vera Gonçalves pela disponibilidade a toda a hora, Sofia Salta e Helena Pereira pela ajuda que disponibilizaram e por relembrar sempre que o cabelo tem que estar atado no laboratório e claro, Vânia Camilo.

Também incluído no grupo dos “mais velhos”, mas sem dúvida o mais imprescindível, João Lobo. Mesmo na Holanda, esteve sempre, sempre mesmo, disponível para o meu projeto e sem ele, não seria possível a concretização do mesmo. Um gigante obrigado.

Quero agora deixar um agradecimento à Iris Garrido Cano, a espanhola que encheu três meses deste percurso de alegria e muito ensinamento. Não podia imaginar que neste momento estaria aqui a

demonstrar este carinho gigante por ela, mas sem dúvida que foi um pilar essencial, que me ensinou muito e que me enche de orgulho! Nunca a vou esquecer e vai ter um lugar especial no meu coração.

Deixo também uma palavra ao Miguel Queirós que mesmo na capital de Portugal, longe de mim, aturou-me um ano em Lisboa e continuou a aturar-me durante este ano no Porto. É uma pessoa incrível que eu só posso desejar o melhor que a vida pode oferecer. Quero também deixar uma palavra de agradecimento à Ana Rita Prada que também me acompanhou em Lisboa e que tornou Lisboa uma cidade mais bonita aos meus olhos.

Quero também expressar o meu agradecimento aos meus amigos que não lidam tanto comigo no dia a dia, mas contribuíram para o sucesso da minha vida profissional e também pessoal, em especial à Mariana Andrade e à Paula Sampaio que estão lá quando preciso.

Embora um pouco de fora de toda esta história que é a “ciência”, quero demonstrar o meu enorme agradecimento à minha família! Só eu sei o quanto eles olham para mim e se sentem orgulhosos por esta caminhada que realizei até aqui. Começo pelo melhor pai do mundo, que me transmite sempre muita confiança e muito positivismo! Que mesmo longe, consegue com uma chamada alegrar o meu dia e me fazer sorrir mesmo que tudo esteja a correr mal. Agradeço de igual maneira à minha mãe que teve sempre uma palavra amiga para me dar, que desejou sempre o meu sucesso e me ajudou nesta luta diariamente. Obrigado por todos os conselhos e por me teres tornado a mulher que sou hoje.

Quero agradecer ao meu irmão de uma forma muito especial, por ser um orgulho para mim, por todo o apoio, por todos os risos e especialmente por ser um confidente. Agradeço aos meus avós, tios, primos pelo papel ativo na minha educação e pela presença nesta caminhada.

RESUMO

O cancro de bexiga é o nono cancro mais incidente no mundo e a décima terceira principal causa de morte por cancro, de acordo com o estudo GLOBOCAN 2018. A maioria dos casos de cancro de bexiga (> 90%) surge no revestimento interno do trato urinário (urotélion) e são designados por carcinoma de células uroteliais. Os subtipos menos comuns são o carcinoma espinocelular, adenocarcinoma, carcinoma de pequenas células e sarcoma. Adicionalmente, o cancro de bexiga pode ser classificado em não músculo-invasivo e em músculo-invasivo. Este primeiro, é responsável por aproximadamente 75% de todos os cancros de bexiga diagnosticados. Apesar destes tumores, geralmente, não representarem uma ameaça à vida dos doentes, a taxa de recorrência é elevada. Por outro lado, tumores músculo-invasivos, que representam cerca de 25% dos casos, são tumores clinicamente mais agressivos, que podem progredir rapidamente, apresentando capacidade de invadir e metastizar para outros órgãos. Assim, há uma necessidade urgente de compreender os mecanismos de progressão do cancro de bexiga, para assim desenvolver novas estratégias de diagnóstico, bem como abordagens terapêuticas efetivas.

Nos últimos anos, o número de estudos na área da genética, epigenética e epitranscriptómica aumentaram drasticamente, principalmente devido ao rápido aprimoramento das tecnologias de sequenciação de alto rendimento de nova geração.

CH Waddington, definiu originalmente o termo Epigenética como o estudo de "mecanismos causais pelos quais os genes do genótipo produzem efeitos fenotípicos". Ao longo do tempo, esta definição sofreu algumas alterações, sendo, hoje, definida como "o estudo de alterações hereditárias na expressão génica que ocorrem independentemente das alterações na sequência primária de ADN". Recentemente foram identificados novos mecanismos de regulação da expressão génica, ao nível do ácido ribonucleico (ARN), designado por epitranscriptómica. Esta refere-se ao estudo de modificações químicas, reversíveis, que podem ocorrer quer em moléculas de ARN, quer em ARN não codificante (ncARN) e em ARN mensageiro (mARN).

A N6-metiladenosina (m6A), metilação da adenosina na posição nitrogénio-6, é a modificação química interna mais abundante nos mARNs dos seres eucarióticos. Esta modificação ocorre, preferencialmente, na sequência DRACH (onde D indica A/G/U; R indica A/G e H indica A/C/U), sendo especificamente enriquecida próximo do codão *stop*, nas regiões 3' não-traduzidas e em grandes exões internos. O seu potencial na regulação da expressão génica foi recentemente explorado e sabe-se que, esta modificação pode afetar diferentes vias do mARN, como a transcrição, *splicing*, exportação do núcleo e tradução. Nas células de mamíferos, esta modificação é catalisada pelo complexo m6A metiltransferase ("*writers*") e pode ser removida pelas desmetilases ("*erasers*"). Além disso, existem proteínas que se ligam diretamente à modificação m6A, mediando a sua função. Estas são conhecidas como "*readers*". Vários estudos revelaram que a metilação do m6A, bem como das suas proteínas reguladoras, desempenha um papel crucial no processo de tumorigénese em diferentes modelos. No entanto, o envolvimento desta modificação no cancro de bexiga é ainda limitado, sendo, portanto, necessário investigar as suas funções no contexto desta neoplasia.

O objetivo do nosso estudo é descobrir o papel da m6A no cancro de bexiga, a fim de perceber quais os mecanismos moleculares subjacentes à agressividade tumoral.

A seleção das proteínas reguladoras da m6A mais informativas para o nosso projeto foi realizada pela análise *in silico* dos dados de ARN-seq de doentes com cancro de bexiga músculo-invasivo, disponíveis na base de dados do TCGA. Esta análise revelou que as principais proteínas reguladoras da m6A desreguladas eram o METTL3, METTL14, VIRMA, WTAP, que formam um "*writer complex*", sendo o METTL3 a única proteína com atividade catalítica, o ALKBH5 e FTO, que têm a capacidade de desmetilar o m6A, e o YTHDF3 que tem como função "*ler*" a marca no citoplasma, determinando se o mARN é traduzido ou degradado.

Assim, foi selecionada (n=120) uma série de tecidos de cancro de bexiga primário, sem qualquer tratamento, dos quais 50% são músculo-invasivo e 50% não músculo-invasivo), bem como uma série de tecidos normais. Em seguida, foi realizada quantificação proteica, por imunohistoquímica. Tal serviu para comparar a expressão em tecidos tumorais e tecidos normais, sendo que, dentro dos tecidos tumorais, a expressão diferencial nos músculo-invasivo e não músculo-invasivo também foi avaliada.

A METTL3, METTL14, VIRMA, ALKBH5 e YTHDF3 apresentam uma expressão significativamente menor nos tumores por comparação com tecidos normais. Além disso, a METTL3 e a METTL14, que formam um heterodímero estável, apresentam uma redução de expressão significativa nos tumores músculo-invasivo, quando comparado com os não músculo-invasivos.

Analisámos a correlação da expressão destas proteínas reguladoras e da m⁶A entre si. Para além disso, observámos que a expressão do *reader* (YTHDF3) e de todos os *writers* estudados se correlacionou positivamente com a expressão da m⁶A. O mesmo foi observado em relação à expressão das *erasers*. Curiosamente, também foram observadas correlações entre a expressão dos *writers* e *erasers*, com exceção da WTAP com ambas as *erasers*, bem como do VIRMA e do FTO. Assim, estes resultados sugerem que a correlação observada entre os *writers* e as *erasers* pode ser explicada através de um feedback compensatório, ou seja, a diminuição dos escritores vai diminuir consequentemente a m⁶A, levando a uma diminuição das *erasers* que desmetilam esta modificação.

A metilação desta modificação no ARN e a expressão das suas proteínas reguladoras, foi avaliada em linhas celulares de bexiga através do ensaio colorimétrico e Western blot, respetivamente. Uma linha celular normal, SVHUC-1, e sete linhas celulares tumorais foram usadas. Relativamente à modificação da m⁶A, não foram observadas diferenças significativas nas diferentes linhas celulares. Em relação às proteínas reguladoras, também não se observaram diferenças significativas para a expressão destas entre as linhas celulares testadas, com exceção do METTL14 que apresentou níveis bastantes variáveis, sendo a linha UMUC3, aquela com valores mais elevados desta proteína.

Nesta sequência, com o objetivo de induzir *in vitro* a ablação da expressão do METTL14, foi realizado o *knockdown* deste gene na linha celular UMUC3, recorrendo ao sistema CRISPR-Cas9. Para avaliar a eficiência desta técnica, realizámos Western blot, onde foi comparada a expressão do METTL14 na linha celular com *knockdown* e na linha UMUC3 normal.

Após confirmar a eficiência da redução da expressão em pelo menos 50% do METTL14, os níveis da modificação da m⁶A foram avaliados, a fim de perceber a importância desta proteína no complexo. Posteriormente, foram realizados ensaios fenotípicos para determinar o impacto da diminuição da sua expressão na linha celular de cancro de bexiga.

Os ensaios *in vitro* demonstraram que a redução da expressão do METTL14 promoveu uma redução de 50% na modificação da m⁶A. Destes, os ensaios de viabilidade e proliferação celular, demonstram que a redução de METTL14 aumenta significativamente a viabilidade e proliferação das células de cancro de bexiga. Além disso, verificámos igualmente, que havia um aumento na capacidade de invasão e migração, comparativamente com as linhas controlo. Em sentido inverso, o *knockdown* do METTL14 traduziu-se numa redução na taxa de apoptose das células tranfectadas.

Em resumo, a expressão das proteínas modeladoras da marca m⁶A encontram-se desregulada no cancro de bexiga. Particularmente, a regulação negativa do complexo METTL3/METTL14 metiltransferase associou-se à progressão do cancro de bexiga não músculo-invasivo para o cancro de bexiga músculo-invasivo.

Estudos anteriores indicam que, embora a METTL14 não possua uma função catalítica, é capaz de formar um heterodímero com a METTL3, sendo necessário para a estabilização e função do complexo. Interações específicas entre o domínio METTL14- MTD14 e o domínio do METTL3- MTD3 são necessárias para a atividade catalítica da METTL3. Na mesma linha, descobrimos que a redução da expressão da METTL14 diminui a atividade do complexo *writer* e, portanto, a capacidade de estabelecer m⁶A nas moléculas de ARN. Estes resultados sugerem que a METTL14 poderá desempenhar

um papel supressor tumoral, estando a redução da sua expressão associada a características celulares tumorais de maior agressividade.

Palavras-chave: Cancro de bexiga, Epitranscriptômica, N6-metiladenosina, METTL14.

ABSTRACT

N6-methyladenosine (m₆A) modification is the most abundant internal chemical modification of mRNAs in eukaryotes. Several studies revealed that m₆A RNA methylation and the associated regulatory proteins, play crucial roles in the tumorigenesis processes of numerous types of cancers. However, knowledge of the mechanistic network between m₆A and bladder cancer (BC) is limited and therefore it is necessary to investigate the functions of this modification.

The aim of our study is to uncover the role of this modification in BC in order to understand the mechanisms associated with tumour aggressiveness.

In silico analysis of TCGA data disclosed altered expression of the major m₆A regulatory proteins, prompting subsequent validation. M₆A, METTL3, METTL14, VIRMA, WTAP, ALKBH5, FTO and YTHDF3 protein expression were evaluated in a series of primary BC (n=120) and normal bladder (n=40) tissues. M₆A RNA methylation and respective regulatory proteins expression were also assessed in bladder cell lines. METTL14 knockdown was performed in UMUC3 cell line using CRISPR-Cas9 system in order to study its relevance in bladder carcinogenesis.

METTL3, METTL14, VIRMA, ALKBH5 and YTHDF3 showed significantly lower expression levels in tumour compared to normal tissues. Moreover, METTL3 and METTL14 (heterodimeric catalytic core) showed a significant reduction in muscle invasive (MIBC) comparing with non-muscle bladder cancer (NMIBC). No differences were apparent for m₆A regulatory proteins' expression among the tested cell lines, except for METTL14, that presented heterogenous levels of this writer in the different cells comparing with normal cell line. The *in vitro* METTL14 downregulation promoted a 50% reduction in m₆A modification. METTL14 knockdown showed increased cell viability/proliferation, invasion and migration capacity, whereas decreased apoptosis was found in the same cells compared with the control.

Our results suggest that METTL14 might have an important role in bladder cancer, and its expression associated with bladder cancer aggressiveness.

Keywords: Bladder cancer, Epitranscriptomic, N6-methyladenosine, METTL14.

TABLE OF CONTENTS

INTRODUCTION	1
MATERIALS AND METHODS	7
<i>In Silico</i> Analysis	7
Patients and Samples Collection.....	7
Immunohistochemical analysis.....	7
Bladder Cancer Cell Lines Studies	9
Protein Extraction and Quantification	9
Western Blot	10
Immunofluorescence analysis.....	11
M ₆ A Quantification.....	11
METTL14 Gene Knockdown	11
Cell Viability and Proliferation Assays	11
Apoptosis evaluation.....	12
Wound Healing Assay	12
Invasion Assay	13
Statistical Analysis.....	13
RESULTS	14
<i>In Silico</i> Analysis	14
Characterization of METTL3, METTL14, VIRMA, WTAP, ALKBH5, FTO, YTHDF3 and m ₆ A immunoexpression in primary tumours	15
Characterization of METTL3, METTL14, VIRMA, WTAP, ALKBH5, FTO and YTHDF3 protein expression in bladder cell lines	18
Cellular localization of m ₆ A and regulatory proteins in cell lines.....	18
RNA m ₆ A methylation quantification in cell lines	19
CRISPR-Cas9 System in UMUC3.....	20
Phenotypic impact of METTL14 in UMUC3 cell line	20
DISCUSSION	22
CONCLUSION AND FUTURE PRESPECTIVES	24
REFERENCES	25

FIGURE INDEX

Figure 1. Worldwide Bladder Cancer incidence. Estimated number of new cases in 2018, worldwide, all cancers, both sexes, all ages. Adapted from (1).....	1
Figure 2. Staging of urothelial carcinoma. Bladder cancer stages are assigned on the basis of tumour invasion through the layers of tissue that constitute the bladder. Adapted from (2).	2
Figure 3. Molecular subtype classification based on RNA subtype classification, pathway information, EMT and CIS signatures, and immune infiltrate analyses. Adapted from (14).	3
Figure 4. N6-methyladenosine (m6A) modification regulation by “writers”, “erasers” and “readers”. This modification is a dynamic and reversible process coordinated by a complex consisting of methyltransferases, METTL3/14, WTAP, RBM15/15B, and KIAA1429 (VIRMA); demethylases FTO and ALKBH5 and “reader” proteins that mediate their function. Teixeira, C. unpublished.....	4
Figure 5. In silico analysis: frequency of alterations in queried genes in TCGA database.	14
Figure 6. Analysis of expression in normal bladder tissue and BC samples (TCGA data, Red box for tumour tissue, n=404; grey box for normal tissue, n=28). Only METTL14 was downregulated in BC.	14
Figure 7. Illustrative images of immunostaining for m6A (a), METTL3 (b), METTL14 (c), VIRMA (d); WTAP (e), ALKBH5 (f), FTO (g) and YTHDF3 (h) in bladder cancer. a Strong (9+) m6A nuclear immunoexpression in bladder cancer; b Strong (9+) METTL3 nuclear immunoexpression in bladder cancer; c Weak/moderate (6+) METTL14 nuclear immunoexpression in bladder cancer; d Weak/moderate (6+) VIRMA nuclear immunoexpression in bladder cancer; e Strong (9+) WTAP nuclear immunostaining in bladder cancer; f Strong (9+) ALKBH5 nuclear immunostaining in bladder cancer; g Strong (9+) FTO nuclear immunostaining in bladder cancer; h Strong (9+) YTHDF3 cytoplasmic immunoexpression in bladder cancer.	16
Figure 8. Characterization of METTL3, METTL14, VIRMA, ALKBH5 and YTHDF3 in normal and bladder cancer tissues by immunohistochemistry. a METTL3 (NMIBC vs MIBC p=0.023; NUT vs NMIBC p=0.005) , b VIRMA (NUT vs NMIBC p=0.003; NUT vs MIBC p=0.006), c METTL14 (NMIBC vs MIBC p=0.049; NUT vs MIBC p=0.003), d ALKBH5 (NUT vs NMIBC p<0.0001; NUT vs MIBC p<0.0001;) and e YTHDF3 (NUT vs NMIBC p=0.003; NUT vs MIBC p=0.006) immunostaining based on h-score (ranges from 0, +1, +2, +3, +4, +6, +9). Qui-square, *p<0.05, **p<0.01, ***p<0.001, ****p<0.0001, ns- non signification. NUT- normal urothelial tumour, NMIBC- non muscle-invasive bladder cancer, MIBC- muscle-invasive bladder cancer.	16
Figure 9. Association between METTL3 protein level and pathological stage. Kruskal-Wallis test (p=0.01).....	17
Figure 10. Characterization of regulatory proteins in bladder cancer cell lines a. METTL3, WTAP, FTO and ALKBH5 protein levels in the same cell lines. b. The expression of METTL14 protein in 7 bladder cancer cell lines in Western blot. SV-HUC1 cell line was used as control. Kruskal-Wallis test.	18
Figure 11. Illustrative images of IF for all tested m6A regulatory proteins. Results are compared to negative control. Photograph taken in microscope Olympus IX51 with a digital camera Olympus XM10 (400x amplification).....	19
Figure 12. Percentage of m6A in mRNA, using the ELISA m6A. Kruskal-Wallis test.	19
Figure 13. Knockdown of METTL14 on the UMUC3 cell line. a. We observed an efficiency in the protein expression of 48% in the condition of 1.5 µl Lipofectamine 3000 and 40% in the condition of 3 µl Lipofectamine 3000. Kruskal-Wallis test, p=0.05. b. Through the colorimetric assay of m6A, we found a reduction in the levels of 62% in the condition of 1.5 µl Lipofectamine 3000 (n.s.) and 73% in	

the condition of 3 μ l Lipofectamine 3000 ($p=0.0407$). Kruskal-Wallis test: $*p < 0.05$, $p=0.0286$. Abbreviations: WT- Will type. 20

Figure 14. Phenotypic impact METTL14 knockdown in UMUC3 cell line. a. in cell viability **b.** in BrdU assay **c.** apoptosis levels after 48 hours (mean \pm SD, $n = 3$) **d.** cell invasion after 24 hours **e.** cell migration after 48 hours. Mann-Whitney U-test: $*p < 0.05$, $**p < 0.01$, $***p < 0.001$ and $****p < 0.0001$ compared to control (WT: UMUC3). Abbreviations: WT- Will Type..... 21

TABLES INDEX

Table 1. Primary antibodies used in Immunohistochemistry	8
Table 2. Clinicopathologic characterization of bladder cell lines	9
Table 3. Primary antibodies used in Western blot and Immunofluorescence	10
Table 4. Clinicopathological parameters of the bladder cancer patients.....	15
Table 5. Correlation between different regulatory proteins. Spearman's rank correlation coefficient (ρ)	17

LIST OF ABBREVIATIONS

3'UTR- 3' untranslated regions
AJCC- American Joint Committee on Cancer
ALKBH5- *alkB* homologue 5
ATCC- American Type Culture Collection
BC- Bladder cancer
BCG- Bacillus Calmette-Guérin
BSA- Bovine serum albumin
BUC- Bladder Urothelial carcinoma
Cis- Carcinoma in situ
DAB- 3,3' – Diaminobenzidine
DAPI- 4',6-diamidino-2-phenylindole
DMSO- Dimethyl Sulfoxide
EDTA- Ethylenediamine tetra acetic acid
EMT- Epithelial-mesenchymal transition
FBS- Fetal Bovine Serum
FFPE- Formalin-fixed and paraffin-embedded
FITC- Fluorescein isothiocyanate
FTO- *Human obesity-associated*
ICC- Immunocytochemistry
IF- Immunofluorescence
IgG- Immunoglobulin G
IHC- Immunohistochemistry
lncRNA- long non-coding RNA
m⁶A- N⁶-Methyladenosine
METTL14- *Methyltransferase-like protein 14*
METTL3- *Methyltransferase-like protein 3*
MIBC- Muscle invasive bladder cancer
MMC- Mitomycin
MMC- Mitomycin C
mRNA- Messenger ribonucleic acids
NAC- Neoadjuvant chemotherapy
ncRNA- non-coding RNA
NMIBC- non-muscle invasive bladder cancer
NUT- Normal urothelial tract
OD- Optical density
PBS- Phosphate buffered saline
PBS- Phosphate-buffered saline
PFA- Paraformaldehyde
PIC- Protein inhibitor cocktail
PVDF- Polyvinylidene fluoride
RBM15/15B- RNA-binding motif proteins 15/15B
RIPA- Radio immune precipitation assay
RNA- Ribonucleic acid
SAM- S-adenosyl-methionine
SDS-PAGE- Sodium dodecyl sulfate polyacrylamide gel electrophoresis

SDS- Sodium dodecyl sulphate
TBS- Tris-buffered saline
TCGA- The Cancer Genome Atlas
TRITC- Tetramethyl rhodamine
TURBT- Transurethral resection of bladder tumour
UCC- Urothelial cell carcinoma
VIRMA- *Virilizer*
WB- Western blot
WHO- World Health Organization
WTAP- *Wilm`s tumour-associated protein*
YTHDF3- *YTH m6A-binding protein 3*
ZC3H13- Zinc finger CCCH domain-containing
 β -ACT- Beta-actin

INTRODUCTION

Bladder cancer (BC) is the tenth most incident cancer worldwide and the thirteenth leading cause of death from cancer, according to GLOBOCAN 2018 study (**Figure 1**) (1). In 2018, 549,000 new cases were diagnosed, and it is expected an increase to 900,700 new cases by 2040 (2, 3). BC has higher incidence and mortality rates in males when compared to females in a 3:1 ratio, approximately. Incidence also correlates positively with age. Furthermore, smoking is the strongest risk factor associated with this disease, with an attributable risk of approximately 50%. Chronic urinary tract infections, exposure to aromatic amines and other carcinogenic substances (such as arsenic in the drinking water) are other common BC drivers (4-6).

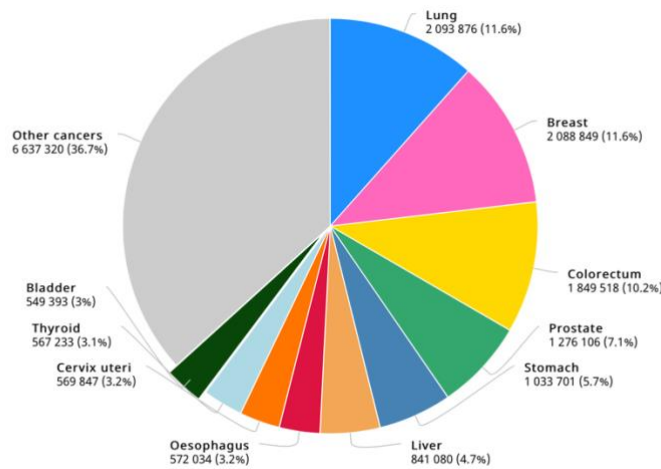


Figure 1. Worldwide Bladder Cancer incidence. Estimated number of new cases in 2018, worldwide, all cancers, both sexes, all ages. Adapted from (1).

Most cases of bladder cancer (>90%) arise from the inner lining of the urinary tract (urothelium) and are commonly designated urothelial cell carcinomas (UCCs). The less-common types are squamous cell carcinoma, adenocarcinoma, small-cell carcinoma and sarcoma (4, 7). Bladder cancer is classified in non-muscle invasive BC (NMIBC) and muscle invasive BC (MIBC). NMIBC accounts for approximately 75% of all diagnosed BC. Although these tumours usually do not represent a survival threat, they frequently recur. Moreover, 10-30% of patients with NMIBC progress to MIBC. The former tumours represent about 25% of the cases are clinically more aggressive tumours that can rapidly progress and metastasize (3, 8). NMIBC and MIBC are staged according with the degree of tumour invasion into the bladder wall. Stage 0 carcinomas, which can be papillary (Ta) or in situ (Tis), and are restricted to the urothelium, and stage 1 (T1) carcinomas, which invade the lamina propria, are grouped as NMIBC. Tumours which invade the superficial muscle (stage T2a) or deep muscle (stage T2b), the peri-vesical fat layer (stage T3) and adjacent organs (stage T4), are grouped as MIBC (**Figure 2**) (9, 10).

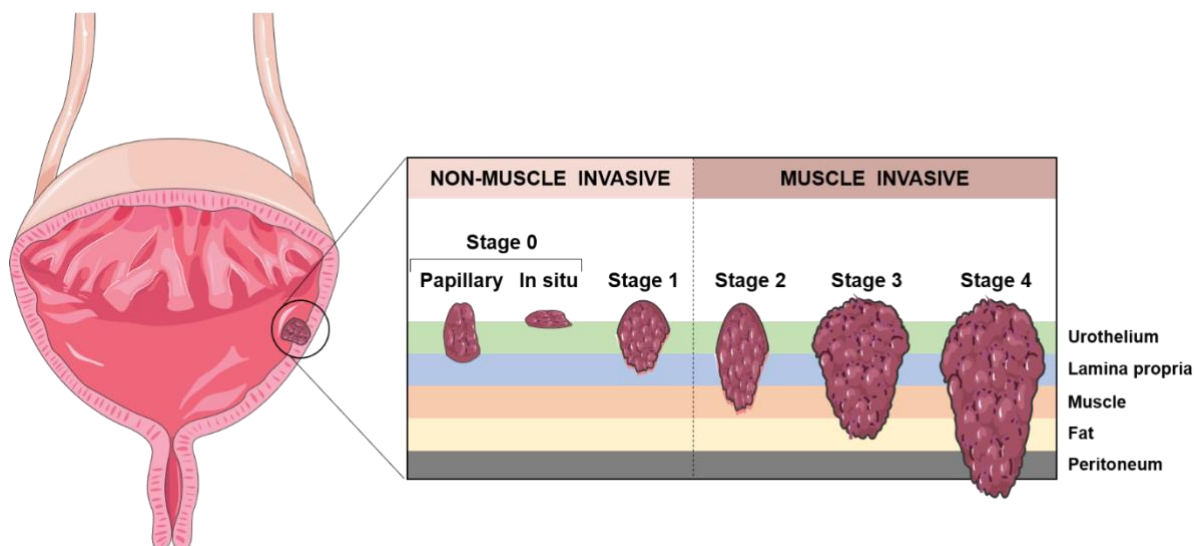


Figure 2. Staging of urothelial carcinoma. Bladder cancer stages are assigned on the basis of tumour invasion through the layers of tissue that constitute the bladder. Adapted from (11).

At the molecular level, several classifications of BC have been, so far, described, and all of them are partially coincident allowing to distinguish two major molecular subtypes: luminal and basal-like BC (10, 12). The Lund classification was the first defined in urothelial carcinoma including NMIBC and MIBC. Five tumour classes were defined with different cell adhesion gene signatures and also different genetic mutations (11). Two other molecular classification systems have been described: The Cancer Genome Atlas (TCGA) and MD Anderson Cancer Center, defined according to messenger ribonucleic acids (mRNA) expression profile studies, included MIBC alone. The group at the University of North Carolina assembled a large dataset showing that tumours could be divided into only two groups, luminal and basal, which is currently the established classification (13).

The most comprehensive classification is provided by TCGA in which muscle-invasive bladder cancer are characterized by multiple TCGA analytical platforms from studies on mRNA, long non-coding RNA (ncRNA) and microRNA's expression, differential epithelial-mesenchymal transition (EMT) status, carcinoma in situ (Cis) scores, histologic features, and survival. The well-known luminal and basal subtypes of BC were stratified into 5 distinct subtypes: luminal-papillary subtype (35%), luminal-infiltrated subtype (19%), luminal subtype (6%), basal-squamous subtype (35%) and neuronal subtype (5%), was recently recognized by others in an independent cohort (**Figure 3**) (14).

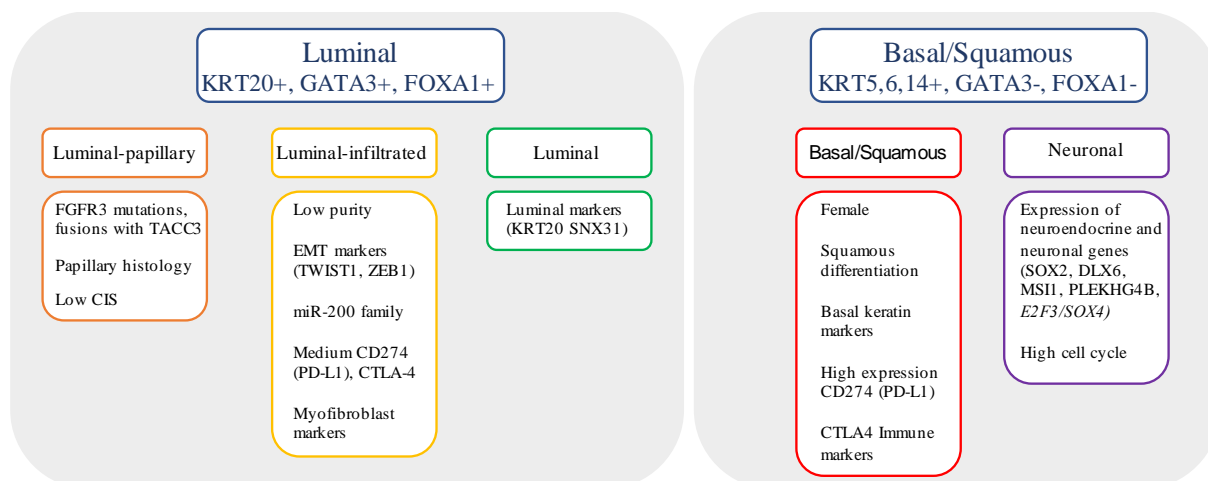


Figure 3. Molecular subtype classification based on RNA subtype classification, pathway information, EMT and CIS signatures, and immune infiltrate analyses. Adapted from (14).

Haematuria (blood cells in urine) is the most common symptom of BC, although it is also associated with various other benign and malignant causes (15). Among benign causes there are trauma, exercise, urinary tract infections, vascular malformations or prostate hyperplasia. Besides BC, malignant causes of haematuria also include kidney and prostate cancer. Because of that, early detection and diagnosis of BC still constitutes a challenge, although urine cytology is performed in high-risk patients for the investigation of the presence of a bladder tumour. Confirmation of presence of tumour cells is performed by cystoscopy (insertion a flexible or rigid scope through the urethra into to bladder), that allows visualization of the inside of the urinary bladder (5). Through this procedure, a biopsy can also be performed, allowing for cytology confirmation. Although, several new tests have been developed, such as bladder tumour associated antigen, the immunocyte assay, nuclear matrixprotein-22 and the Uro Vysion assay, none of them is commonly used in clinical practice due to relatively low sensitivities and/or specificities and the diagnosis is performed by Cytology and/ or histology (4).

The standard treatment for early-stage BC patients is the transurethral resection of bladder tumour (TURBT), that might be followed by intravesical therapy, either with a chemotherapeutic agent (Mitomycin C - MMC) or immunotherapy (bacillus Calmette-Guérin - BCG). Advanced cancers may require removal of the entire bladder (cystectomy), radiation and/or systemic chemotherapy treatments (11, 16). As the recurrence rate for this type of cancer is very high, some patients have to endure various surgeries through time, increasing their morbidity and also the financial costs related with BC treatment.

Therefore, there is an urgent need to understand the mechanisms of bladder cancer progression for the development of new diagnostic and therapeutic strategies. This is of great importance for clinical patient's management. In the last few years, the number of genomic, epigenomic and epitranscriptomic studies have increased dramatically, mostly due to the rapid improvement of high-throughput DNA sequencing technologies.

C. H. Waddington originally defined the term Epigenetics as the study of "causal mechanisms by which genes of the genotype bring about phenotypic effects" (17). However, this initial definition evolved over time, being less focused on the genotype, and more implicated in a wide variety of biological processes. Thus, the current definition of epigenetics is "the study of heritable changes in gene expression that occur regardless of changes in the primary DNA sequence" (18). The main epigenetic molecular mechanisms are grouped into four main groups: DNA methylation, histone post-translational modifications or chromatin remodelling, histone variants, and ncRNAs regulation (19).

Recently, a new layer of gene expression regulation at the RNA level was identified. Epitranscriptomic refers to the study of reversible chemical modifications that may occur in RNA

molecules, including ncRNA and mRNA (20-22). N6-methyladenosine (m⁶A), methylation of the adenosine base at the nitrogen-6 position, is the most abundant internal chemical modification of mRNAs and in long non-coding RNA (lncRNA) in eukaryotes. Its potential in gene expression regulation has been recently explored (22).

This modification occurs preferentially in DRACH sequence (where D denotes A/G/U; R denotes A/G and H denotes A/C/U) (23, 24). The m⁶A is specifically enriched near the stop codon, in the 3' untranslated regions (3'-UTR), and within long internal exons, thereby affecting different steps of mRNA's life, such as transcription, splicing, nuclear export and translation (24). In mammalian cells, this modification is catalysed by the m⁶A methyltransferase complex ("writers") and can be removed by m⁶A demethylases ("erasers"). There are also proteins that bind directly to the m⁶A mark and mediate its function, known as "readers" (Figure 4) (25-27).

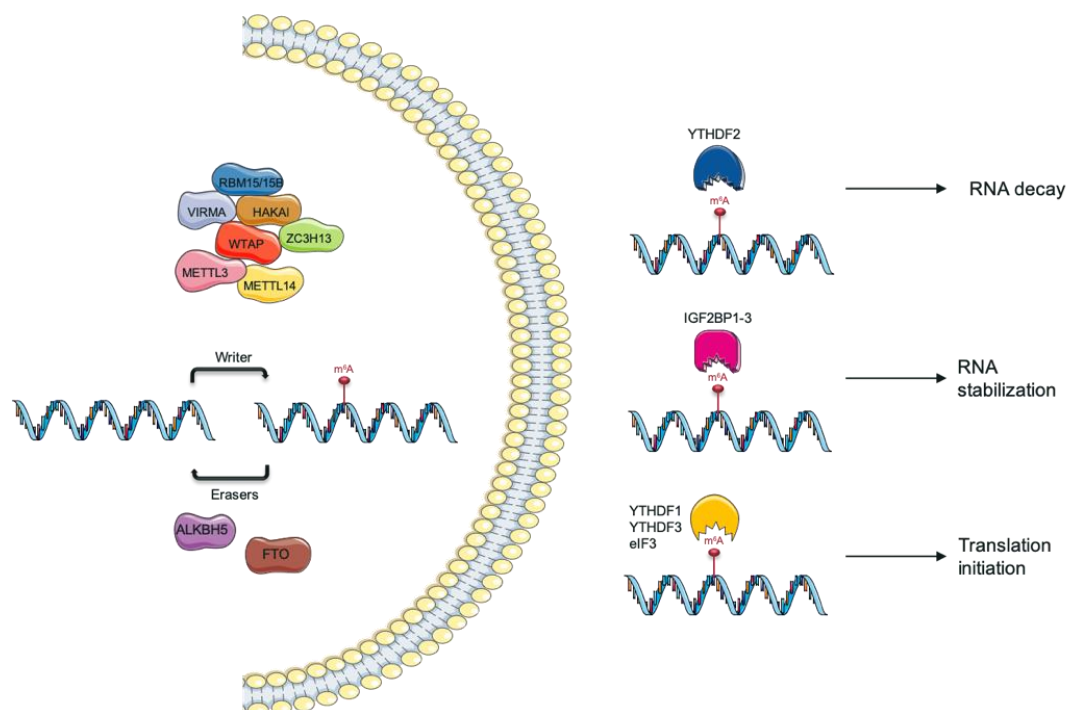


Figure 4. N6-methyladenosine (m⁶A) modification regulation by “writers”, “erasers” and “readers”. This modification is a dynamic and reversible process coordinated by a complex consisting of methyltransferases, METTL3/14, WTAP, RBM15/15B, and KIAA1429 (VIRMA); demethylases FTO and ALKBH5 and “reader” proteins that mediate their function. Teixeira, C. *unpublished*.

The m⁶A modification is catalysed by the methylase complex composed by the methyltransferase-like 3 and 14 proteins (METTL3 and METTL14) and their cofactors: Wilm’s tumour-associated protein (WTAP), Virilizer (KIAA1429/VIRMA), RNA-binding motif proteins 15/15B (RBM15/15B), and zinc finger CCCH domain-containing protein 13 (HAKAI and ZC3H13) (28).

METTL3 and METTL14 constitute a heterodimer that induces m⁶A synergistically. Although METTL3 was already reported to play a central role in complex stability, data is lacking for METTL14 (28, 29). WTAP is a regulatory subunit required for the nuclear complex, since it positions METTL3 and METTL14 to allow its connection/functionality, and also recruits other factors to the methyltransferase complex (26, 27). VIRMA recruits the methyltransferase core components - METTL3, METTL14 and WTAP - via WTAP in a RNA-independent manner, and rather favours mRNA methylation near the 3'-UTR and stop codon regions (30). The RNA binding protein RBM15 and its

homolog RBM15b, preferentially bind to RNA's U-rich regions, recruiting the m⁶A complex through interaction with METTL3 in a WTAP-dependent manner (22).

Furthermore, m⁶A modification can be demethylated by the human obesity-associated protein (FTO), which is conserved among eukaryotes and it is one of the RNA demethylases that belongs to the ALKB family. AlkB homologue 5 (ALKBH5) is another demethylase that binds to single stranded nucleic acids and therefore differs from the other members of the ALKB protein family (31, 32). These proteins ensure a balanced equilibrium of m⁶A modification.

The identified "readers" of m⁶A are YTH domain family proteins. Specifically, YTH m⁶A-binding protein 3 (YTHDF3) cooperates with YTHDF1 (promoting translation) and YTHDF2 (promoting mRNA degradation) affecting cytoplasmic metabolism of methylated mRNAs, and translation (33).

Several studies showed that m⁶A RNA methylation and the associated regulatory proteins are implicated in cancer, including leukaemia, breast, lung, brain, liver, cervical and endometrial cancer. However, knowledge of the mechanistic network between m⁶A and BC is rather limited, being necessary to further investigate the role of this modification in this malignancy. Hence, the deregulation of the main players: METTL3, METTL14, WTAP, VIRMA, FTO, ALKBH5 and YTHDF3 was also investigated.

Aims

The m₆A modification and the associated regulatory proteins (METTL3, METTL14, WTAP, VIRMA, FTO, ALKBH5 and YTHDF3) play critical roles in the pathogenesis of various types of cancers, however, the role of these proteins remains poorly explored in bladder cancer. Thus, studying the role of this modification may uncover mechanisms associated with BC aggressiveness.

Specifically, the following tasks were set:

1. Evaluate m₆A, METTL3, METTL14, WTAP, VIRMA, ALKBH5, FTO and YTHDF3 expression in a patient's cohort of BC patients diagnosed with primary tumour prior to any treatment. Proteins' s expression was also evaluated in a series of normal bladder tissues.
2. Compare the immunoexpression findings with clinical and pathological features of bladder cancer patients.
3. Assess m₆A RNA methylation expression levels and respective players protein expression and cellular localization in eight bladder cell lines to molecularly characterize and identify the best *in vitro* model for further studies.
4. Modulate the most promising m₆A regulator using CRISPR-Cas9 system, in order to study its relevance in bladder carcinogenesis.

MATERIALS AND METHODS

In Silico Analysis

To evaluate the expression of m⁶A writers, erasers and readers, the online platform cBio-Portal was used for *in silico* analysis. The Cancer Genome Atlas (<http://cancergenome.nih.gov>) database was selected to determine which subunit may play the crucial role of m⁶A deregulation in BC.

For this, the online platform cBio-Portal for Cancer Genomics was used (34), with the user-defined entry gene set “*METTL3*, *METTL14*, *VIRMA*, *WTAP*, *ALKBH5*, *FTO* and *YTHDF3*”.

GEPIA web server was used for analysing the RNA sequencing expression data of bladder tumours and normal samples from the TCGA and GTEx projects using a standard processing pipeline: $|\log_2FC|$ Cut-off = 1 ; p -value cut-off = 0.01 (35).

Patients and Samples Collection

One hundred twenty (sixty of NMIBCs and others sixty of MIBCs) formalin-fixed and paraffin-embedded tissues were collected from the archives of the department of pathology of Portuguese Oncology Institute of Porto.

These samples are representative of primary bladder urothelial carcinomas (BUCs), without any prior treatment, and diagnosed between 1997 and 2005 at Portuguese Oncology Institute- Porto, Portugal.

Additionally, for control purposes, 40 tissue samples of normal urothelial tract (NUT), originating from nephrectomy specimens of patients with kidney cancer.

This study was approved by the ethics committee (Comissão de Ética para a Saúde) of the Portuguese Oncology Institute of Porto (CES-IPO 372/2017).

Clinical files and pathology reports were reviewed. All histological slides (of primary tumours) were reviewed by a pathologist and tumours were reclassified in light of the most recent 2016 *World Health Organization (WHO) Classification of Tumours of the Urinary System and Male Genital Organs* (36). Staging was performed according to the 8th edition of the *American Joint Committee on Cancer (AJCC) staging manual* (37).

Immunohistochemical analysis

Immunohistochemistry (IHC) analysis for m⁶A modification, m⁶A writers *METTL3*, *METTL14*, *VIRMA* and *WTAP*, erasers *ALKBH5* and *FTO*, and reader *YTHDF3* was performed using the Novolink™ Max Polymer Detection System (Leica Biosystems, Germany). Four μm thick sections were cut and placed in coated slides. In short, after sections deparaffinization (through xylene) and hydration (through a graded alcohol series), antigen retrieval was accomplished by microwave at 800 W or water bath at 95°C in specific buffer, depending on the protein studied (**Table 1**). Then, endogenous peroxidase activity was inhibited with freshly prepared 0.6% hydrogen peroxide solution for 20 minutes, and the unspecific bindings were blocked with horse serum (1:50 dilution) for 20 minutes, at room temperature (RT) in a humidified chamber. Incubation of the primary antibody was performed overnight at 4°C, at a dilution dependent on the specific antibody (**Table 1**). Afterwards, slides were washed in tris-buffered saline (TBS) solution with 0.1% Tween 20, and incubated with post primary, followed by polymer (30 minutes each). Slides were therefore washed, developed with 3,3'-Diaminobenzidine tetrahydrochloride chromogen (DAB, Sigma-Aldrich™, Germany) and counterstained with haematoxylin (Leica Biosystems Richmand, USA). Finally, after dehydration and

diaphanization, slides were mounted in Entellan® (Merck-Millipore, Germany). Appropriate positive controls were used for each antibody and can be consulted in **Table 1**.

The semi-quantitative analysis of immunoexpression was performed by an experienced pathologist and categorized according intensity (between 0-3) and percentage (between 0-100%, and later categorized between 0-3). The score for intensity was performed as score 0 (absent immunoexpression), score 1+ (immunoexpression less intense than in control tissue), score 2+ (immunoexpression similar to control tissue), score 3+ (immunoexpression more intense than in control tissue). The score for percentage was classified in: score 0 (<1% of immunoreactive cells), score 1+ (<50% of immunoreactive cells), score 2+ (50-75% of immunoreactive cells) and score 3+ (75-100% of immunoreactive cells). The final staining score was calculated by multiplying intensity and percentage score, resulting in a score value ranging from 0 to 9+. Pictures were taken in a microscope Olympus BX41 with digital camera Olympus U-TV0.63XC using Cell A software.

Table 1. Primary antibodies used in Immunohistochemistry

Antibodies	Vendor	Catalog number	Positive control	Antigen retrieval	Primary antibody dilution
Anti-METTL3 [EPR18810]	Abcam, Cambridge, United Kingdom	ab195352	Normal testicle	EDTA buffer microwave (1mM, pH=8)	1:500 overnight 4°C
Anti- METTL14 [CL4252]	Abcam, Cambridge, United Kingdom	ab220031	Normal testicle	Citrate buffer microwave (10mM, pH=6)	1:750 overnight 4°C
Anti- WTAP [EPR18744]	Abcam, Cambridge, United Kingdom	ab195380	Normal testicle	EDTA buffer microwave (1mM, pH=8)	1:500 overnight 4°C
Anti-VIRMA/ Virilizer	Cell Signaling Technology, United States, USA	88358	Normal testicle	Citrate buffer microwave (10mM, pH=6)	1:200 overnight 4°C
Anti-FTO [5-2H10]	Abcam, Cambridge, United Kingdom	ab92821	Normal testicle	Citrate buffer microwave (10mM, pH=6)	1:500 overnight 4°C
Anti- ALKBH5	Proteintech Europe, United Kingdom	16837-1-AP	Normal testicle	Citrate buffer microwave (10mM, pH=6)	1:500 overnight 4°C
Anti- YTHDF3	Abcam, Cambridge, United Kingdom	ab103328	Breast cancer	EDTA buffer water bath (1mM, pH=8)	1:100 overnight 4°C
Anti-N6-methyladenosine (m6A)	Abcam, Cambridge, United Kingdom	ab190886	Normal brain	EDTA buffer water bath (1mM, pH=8)	1:750 overnight 4°C

Bladder Cancer Cell Lines Studies

Seven bladder cancer, MGHU3, RT112, 5637, J82, T24, UMUC3, TCCSUP, and one bladder cell line SV-HUC1 from American Type Culture Collection (ATCC), were used for m⁶A players' characterization (**Table 2**).

All culture media were supplemented with 10% Fetal Bovine Serum (FBS, Biochrom, MERK, Germany) and 1% penicillin/streptomycin (GIBCO®, Invitrogen, USA). Cells were maintained at 37°C with 5% CO₂ and routinely tested for *Mycoplasma sp.* contamination using a PCR-based universal mycoplasma detection kit (PCR Mycoplasma Detection Set, Clontech Laboratories, Oxford, UK).

To perform cellular assays, sub-confluent cells were detaching with trypsin at 37°C (Gibco, Invitrogen). Trypsin was inactivated with media 10% FBS, collected and centrifuged at 1,200 rpm during 5 minutes. Cells were resuspended in fresh medium and 10 µl of cell suspension were collected for cell counting with 10 µl of Trypan Blue in the Neubauer chamber. Cell density was then calculated to the different assays.

Table 2. Clinicopathologic characterization of bladder cell lines

Cell Line	Type	Grade ^a	Stage ^a	Subtype ^a	Gender	Media
SV-HUC1	normal	n/a	n.a.	n.a.	male	F12-K
MGHU3	tumour	G1	pTa/T1	luminal	male	DMEM
RT112	tumour	G2	pTa	luminal	female	RPMI
5637	tumour	G2	pTx	mixed	male	RPMI
J82	tumour	G3	pT3	basal	male	MEM
T24	tumour	G3	pTa	basal	female	RPMI
UMUC3	tumour	G3	pT2- T4	basal	male	DMEM
TCCSUP	tumour	G4	pTx	basal	female	MEM

n.a.- not applicable

a- according to (38)

Protein Extraction and Quantification

Total protein was extracted from cells, in triplicates, using the radioimmunoprecipitation assay buffer (RIPA) (Santa Cruz Biotechnology Inc., USA) complemented with 10% of protein inhibitor cocktail (PIC). After 15 minutes in the ice, the samples were centrifuged at 13,000 rpm during 30 minutes at 4°C and the supernatant was collected.

Subsequently, quantified using a Pierce BCA Protein Assay Kit (Thermo Scientific Inc., USA), according to manufacturer's instructions.

Western Blot

Briefly, 30 µg of protein from each cell line was resuspended in loading buffer, denatured at 95°C for 5 minutes, and loaded in 8% polyacrylamide gel where they were separated by size through sodium dodecyl sulphate-polyacrylamide gel electrophoresis (SDS-PAGE) at 120 V for RT. Then, proteins were transferred to 0.2 µm polyvinylidene fluoride (PVDF) membranes (Bio-Rad Laboratories Inc., Hercules, CA, USA) using 25 mM Tris-base/glycine buffer and a Trans-Blot Turbo Transfer system (Bio-Rad) at 25 V and 1.3 mA for 15 minutes. After that, membranes were blocked with 5% bovine serum albumin (BSA; Santa Cruz, USA) or 5% dry milk in TBS with 0.1% Tween (TBS-T, pH=7.6), and then incubated with primary antibody (**Table 3**). After incubation, membranes were incubated with secondary antibody coupled with horseradish peroxidase (Bio-Rad, USA), for 1 hour at RT. To ascertain equal loading of protein, the membranes were incubated with an endogenous control antibody. Quantification was performed using band densitometry analysis from the ImageJ software (version 1.6.1, National Institutes of Health), by comparing the specific protein band intensity with the loading control beta-actin (β -ACT).

Table 3. Primary antibodies used in Western blot and Immunofluorescence

Antibodies	Vendor	Catalog number	Western-blot dilution	Primary antibody: incubation time	Secondary antibody specie	Blocked	IF dilution
Anti-METTL3	Abcam, Cambridge, United Kingdom	ab195352	1:1000	1h at RT	Anti-rabbit	BSA 5%	1:250
Anti-METTL14	Abcam, Cambridge, United Kingdom	ab220031	1:1000	1h at RT	Anti-mouse	BSA 5%	1:50
Anti-WTAP	Abcam, Cambridge, United Kingdom	ab195380	1:1000	1h at RT	Anti-rabbit	BSA 5%	1:100
Anti-VIRMA / Virilizer	Cell Signaling Technology, United States, USA	88358	n.a.	n.a.	n.a.	n.a.	1:100
Anti-FTO	Abcam, Cambridge, United Kingdom	ab92821	1:1000	1h at RT	Anti-mouse	Milk 5%	1:100
Anti-ALKBH5	Proteintech Europe, United Kingdom	16837-1-AP	1:1000	1h at RT	Anti-rabbit	Milk 5%	1:500
Anti-YTHDF3	Abcam, Cambridge, United Kingdom	ab103328	n.a.	n.a.	n.a.	n.a.	1:250
β-Actin	Sigma-Aldrich	A1978	1:10,000	1h at RT	Anti-mouse	BSA 5%	n.a.

n.a. – not applicable; RT – room temperature

Immunofluorescence analysis

M₆A, METTL3, METTL14, VIRMA, WTAP, ALKBH5, FTO and YTHDF3 protein expression and cellular localization assessed by immunofluorescence (IF). Cells were seeded in coverslips in 24-well plates at 25,000 cells/well previously optimized concentration and allowed to adhere at 37°C, 5% CO₂ overnight. In the next day, cells were fixed 4% paraformaldehyde (PFA) for 10 minutes and permeabilized with 0.25% Triton X-100 solution in phosphate-buffer saline (PBS) for 15 minutes. After that, cells were blocked with 5% BSA for 30 minutes, followed by primary antibody incubation at specific dilution (**Table 3**), overnight at RT.

Following primary antibody, cells were incubated with secondary antibody anti-rabbit immunoglobulin G (IgG) (Alexa Fluor™ 488 goat, A11008; Invitrogen, USA) or anti-mouse IgG-fluorescein isothiocyanate (FITC goat SLB4878, Sigma-Aldrich™) for 1 hour, at RT (**Table 4**). Then, nuclear stained was performed with 4',6-diamidino-2-phenylindole (DAPI) (AR1176, BOSTER Biological Technologies, China) in mounting medium. Pictures were taken in fluorescence microscope Olympus IX51 with a digital camera Olympus XM10 using CellSens software (Olympus, Japan) (400x magnification).

M₆A Quantification

RNA was extracted from cell lines by TripleXtractor (GRiSP®, Portugal) according to manufacturer's recommend protocol. To detect m₆A levels, m₆A RNA Methylation Quantification Kit (ab185912; Abcam) was used as the recommended. In this assay, the m₆A is detected using capture and detection antibodies. The detected signal is enhanced and then quantified using colorimetric methodology by reading the absorbance in a microplate spectrophotometer. The amount of m₆A is proportional to the optical density (OD) intensity measured.

METTL14 Gene Knockdown

After protein analysis by Western blot, UMUC3 cell line was chosen to perform METTL14 gene knockdown by plasmids carrying the CRISPR-Cas9 system containing a guide RNA sequence targeting METTL14 (GenScript, Piscataway, NJ). For plasmid transfection, Lipofectamine® 3000 reagent (Invitrogen, USA) was used according to manufacture instructions, followed by selection of cells which incorporated the CRISPR-Cas9 system with 1 µg of puromycin for each 1 mL of DMEM cell culture medium (Sigma).

After selection, cells were expanded, and total protein was extracted in order to confirm METTL14 protein downregulation. UMUC3 will type cells were used as controls for Western blot analysis.

Cell Viability and Proliferation Assays

The effects on cell viability was assessed by MTT assay (Sigma-Aldrich, Germany). Viable cells incorporate MTT solution and the mitochondrial enzyme succinate-dehydrogenase convert them into a purple coloured formazan product.

Cell proliferation was measured by using the Cell Proliferation ELISA BrdU assay (Roche Applied Sciences), based on DNA synthesis analysis. This is a colorimetric immunoassay where 5-bromo-2'-deoxyuridine (BrdU), a pyrimidine analogous, is incorporated in placed of pyrimidine into

the newly synthesized DNA. The quantity of BrdU incorporated into cells is directly correlated to the number of proliferating cells.

Cells were plated into 96 well plates in complete DMEM Medium at density of 6,000 cells/well and incubated overnight, at 37°C in 5% CO₂. Then, cells were maintained with DMEM 1% FBS, from 0 hours until 48 hours.

In MTT assay, the culture medium was removed, and cells were incubated during 1 hour at 37°C with 5 µg/mL MTT solution in complete culture medium. After that, formazan crystals formed were dissolved in dimethyl sulfoxide (DMSO) and spectrophotometric measurement was done at 540nm (reference wavelength: 655 nm) in a microplate reader (Fluostar Omega, BMG Labtech, Germany). DMSO was used as blanks to correct the OD values, and OD obtained for 48 hours was normalized for the 0 hours' time point.

For BrdU assay, cells were incubated with 20 µM BrdU labelling solution for 12 hours. After removing labelling medium, cells were fixed for 30 minutes at room temperature with FixDenat solution. This solution induces DNA denaturation necessary to allow conjugated antibody binding to the incorporated BrdU. Then, FixDenat was removed, and anti-BrdU-POD antibody (dilution 1:100) was added to detect the incorporated BrdU in DNA. After 90 minutes, at room temperature, the antibody was removed, and cells were rinsed 3 times with 1X PBS. The immune complex formed was detected by adding 100 µl/well of substrate solution and incubated for 5-10 minutes, until colour development. Then, the reaction was stopped with 1 M H₂SO₄ added to each well, and the reaction product was quantified in a microplate reader (Fluostar Omega, BMG Labtech, Germany) by measuring absorbance at 450 nm (reference wavelength: 690 nm). The OD values obtained for 48 hours was normalized for the 0 hours` time point.

The results represent the mean of three independent experiments, each one in triplicate, and were analysed using a GraphPad Software.

Apoptosis evaluation

In order to complement cell behaviour studies, apoptosis assay were performed. Briefly, 4x10⁴ cell/well of cells were seeded on 24-well plates and incubated during 48 hours at 37°C and 5% CO₂. After 48 hours, the Cell-APOPercentage™ apoptosis assay kit (Biocolor, United Kingdom) were performed according the manufacturing instructions. Then, cells were incubated with 300 µl/well of APOPercentage™ dye solution at ratio 1:20 respectively, during 30 minutes at 37°C. Next, cells were washed with PBS 1X and detached from well plate with TrypLe™ Express (GBICO, Invitrogen, USA) at 37°C. After that, APOPercentage™ dye release reagent was added and plate were vigorously agitated during 15 minutes, following colorimetric measurement at 550 nm with 620 nm reference filter (Fluostar Omega, BMG Labtech, Offenburg, Germany). The H₂O₂ was used as a positive control. The OD obtained for apoptosis assay was normalized for the OD obtained by viability assay at the same time point.

Wound Healing Assay

The wound-healing assay is one of the earliest developed methods to study directional cell migration *in vitro* and, mimics cell migration during wound healing *in vivo*.

Cells were seeded (6-well plate) in complete DMEM Medium at an optimal density to obtain at least 95% of confluence in the next 24 hours, and incubated at 37°C, 5% CO₂. In the next day, the culture medium was removed, and two “wounds” were made by manual scratching with a 200 µL pipette tip for each condition. Then, the wells were washed with 1X PBS in order to remove detached cells in

wound and incubated with complete cell medium (DMEM 1% FBS). The wound areas were photographed in two specific sites at 40x magnification using an Olympus IX51 inverted microscope equipped with an Olympus XM10 Digital Camera System. The photos were taken at regular time points (between 0 and 48 hours) until wound closure. The relative migration distance (5 measures by wound) was calculated with the following formula: relative migration distance (%) = $(A-B)/C \times 100$, where A is the width of cell wound at 0 hours incubation, B is the width of cell wound after specific hours of incubation, and C is the width mean of cell wound for 0 hours of incubation. For relative migration distance, the results were analysed using the beWound - Cell Migration Tool (Version 1.5) (developed by A.H.J. Moreira, S. Queirós and J.L. Vilaça, Biomedical Engineering Solutions Research Group, Life and Health Sciences Research Institute - University of Minho; available at <http://www.besurg.com/sites/default/files/beWoundApp.zip>). At least three independent experiments were performed.

Invasion Assay

Cell invasion was evaluated by using 24-well BD BioCoat Matrigel Invasion Chambers, with 8µm pore size membranes (BD BioSciences, USA). These invasion chambers allow to compare the *in vitro* cells invasive behaviour in specific conditions. Invasive cells are able to detach themselves and invade through the Matrigel Matrix. On the other hand, the thin layer of Matrigel Matrix mimics a basal membrane that occludes the pores of the membrane, blocking non-invasive cells from migrating through the membrane.

After BD Matrigel Chambers rehydration between 30 minutes and 2 hours with serum free culture media at 37°C, cells at a density of 30,000 cells/insert were seeded in complete culture medium supplemented with 1% FBS and incubated during 24 hours at 37°C in 5% CO₂. Then, the non-invading cells were removed by with swab and invaded cells were methanol fixed, DAPI stained and counted in a fluorescence microscope Olympus IX51 with a digital camera Olympus XM10 using CellSens software. The invasion was calculated as % of cell invasion normalized for the control condition.

Statistical Analysis

Statistical analysis was performed using the GraphPad Prim 7.0 software (GraphPad Software Inc., Chicago IL, USA) and IBM® SPSS® Statistic software version 23 (IBM-SPSS Inc., La Jolla, CA; USA). Significance level was set at $p < 0.05$. Non-parametric Mann-Whitney U test were used to compare two groups. For comparison between three or more groups, non-parametric Kruskal-Wallis test was used, followed by Mann-Whitney U test for pairwise comparisons and Bonferroni's correction, when applicable. Differences in METTL3, METTL14, VIRMA, WTAP, ALKBH5, FTO, YTHDF3 and m6A immunoexpression between normal urothelial tract and BUCs tissues was assessed by Chi-square or Fisher's exact test. Correlation between continuous variables was assessed with Spearman's (rs) non-parametric correlation test.

P-values were considered statistically significant when inferior to 0.05. Significance is shown vs. the respective control and depicted as follows: * $p \leq 0.05$, ** $p < 0.01$, *** $p < 0.001$, **** $p < 0.0001$ and $ns p > 0.05$ (non-significant).

RESULTS

In Silico Analysis

We first aimed to characterize the expression of m⁶A regulatory proteins using available data at the online platform cBio-Portal for Cancer Genomics was used (34), with the user-defined entry gene set “*METTL3*, *METTL14*, *VIRMA*, *WTAP*, *ALKBH5*, *FTO* and *YTHDF3*”.

The database includes tumours samples of 413 patients with MIBC although node negative. Seventy-four % were male whereas 26% were females with a median age at diagnosis of 61 years (Figure 5).

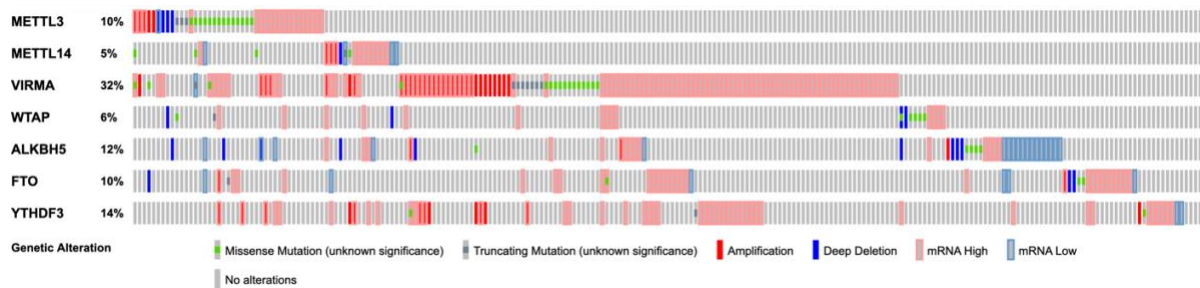


Figure 5. *In silico* analysis: frequency of alterations in queried genes in TCGA database.

In silico analysis showed that m⁶A players displayed different molecular alterations in MIBC. From all the known RNA-modification enzymes related with m⁶A modifications, *VIRMA* was the most frequently altered gene in these tumours. Furthermore, only *METTL14* mRNA expression was significantly downregulated in bladder cancer compared to the normal bladder tissue (Figure 6).

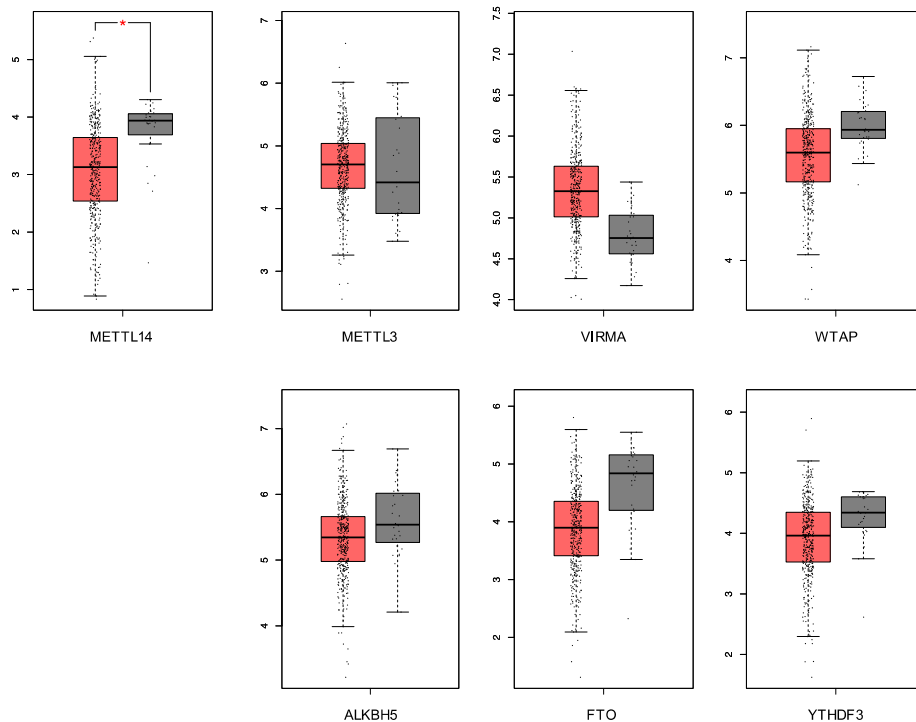


Figure 6. Analysis of expression in normal bladder tissue and BC samples (TCGA data, Red box for tumour tissue, n=404; grey box for normal tissue, n=28). Only *METTL14* was downregulated in BC.

Since, no data is available for NMIBC and validation is lacking for MIBC, these genes were studied in a patient's cohort of IPOPorto.

Characterization of METTL3, METTL14, VIRMA, WTAP, ALKBH5, FTO, YTHDF3 and m⁶A immunoexpression in primary tumours

Immunohistochemistry assay was performed to evaluate proteins' expression in IPOPorto bladder tissues. For this, a total of 120 patients, comprising 60 (50%) NMIBC and 60 (50%) MIBC were included in this study. Additionally, normal urothelial obtained from 40 renal cell carcinoma patients submitted to nephrectomy without urothelial cancer was also analysed (**Table 4**).

Table 4. Clinicopathological parameters of the bladder cancer patients

CLINICOPATHOLOGICAL FEATURES	BUC	NUT
Patients, n	120	40
Gender, n (%)		
Male	93 (77.5%)	25 (62.5%)
Female	27 (22.5%)	15 (37.5%)
Median age, years (range)	69 (43-89)	63 (40-87)
MIBC and NMIBC, n (%)		
Muscle Invasive	60 (50%)	n.a.
Non-Muscle Invasive	60 (50%)	n.a.
Pathological stage, n (%)		
pTa	11 (9.2%)	n.a.
pT1	29 (24.2%)	n.a.
pT2	44 (36.7%)	n.a.
pT3	22 (18.3%)	n.a.
pT4	10 (8.3%)	n.a.
pTx	4 (3.3%)	n.a.

BUC: bladder urothelial carcinomas; NUT: normal urothelial tract

Nuclear expression was observed for all tested proteins, excepting for the “reader” YTHDF3, which exclusively showed a cytoplasmic expression (**Figure 7**).

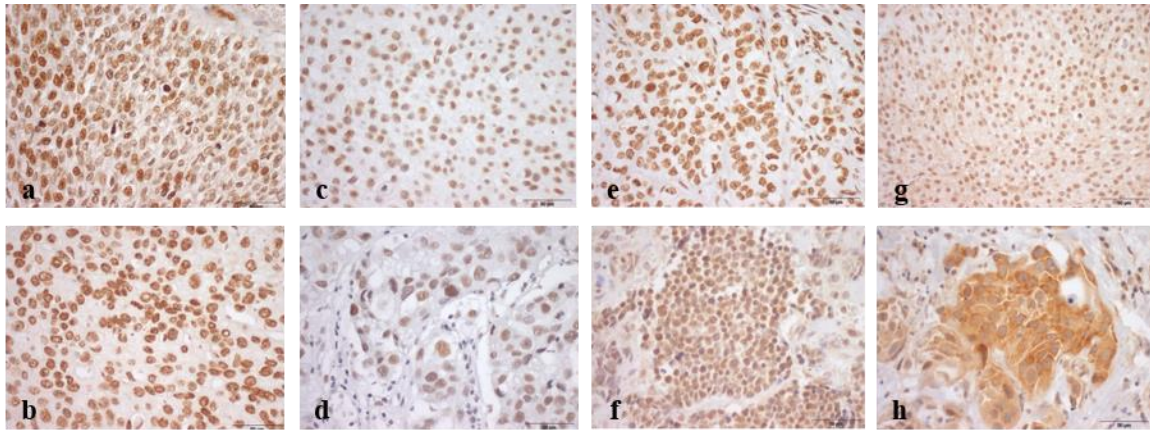


Figure 7. Illustrative images of immunostaining for m⁶A (a), METTL3 (b), METTL14 (c), VIRMA (d); WTAP (e), ALKBH5 (f), FTO (g) and YTHDF3 (h) in bladder cancer. **a** Strong (9+) m⁶A nuclear immunoeexpression in bladder cancer; **b** Strong (9+) METTL3 nuclear immunoeexpression in bladder cancer; **c** Weak/moderate (6+) METTL14 nuclear immunoeexpression in bladder cancer; **d** Weak/moderate (6+) VIRMA nuclear immunoeexpression in bladder cancer; **e** Strong (9+) WTAP nuclear immunostaining in bladder cancer; **f** Strong (9+) ALKBH5 nuclear immunostaining in bladder cancer; **g** Strong (9+) FTO nuclear immunostaining in bladder cancer; **h** Strong (9+) YTHDF3 cytoplasmic immunoeexpression in bladder cancer.

Overall, METTL3, METTL14, VIRMA, ALKBH5 and YTHDF3 immunoeexpression differed significantly between tumour and normal tissues. Specifically, METTL3 ($p=0.0030$), METTL14 ($p=0.0019$), VIRMA ($p=0.0081$), ALKBH5 ($p<0.0001$) and YTHDF3 ($p=0.0107$) showed significantly lower expression in bladder cancer compared with normal tissues. Moreover, METTL3 and METTL14 (heterodimeric catalytic core) showed a significant reduction in muscle invasive tumours comparing with NMIBC ($p=0.0227$ and $p=0.0489$, respectively) (**Figure 8**). Nonetheless, no significant differences were apparent regarding m⁶A, WTAP and FTO expression among the three studied groups.

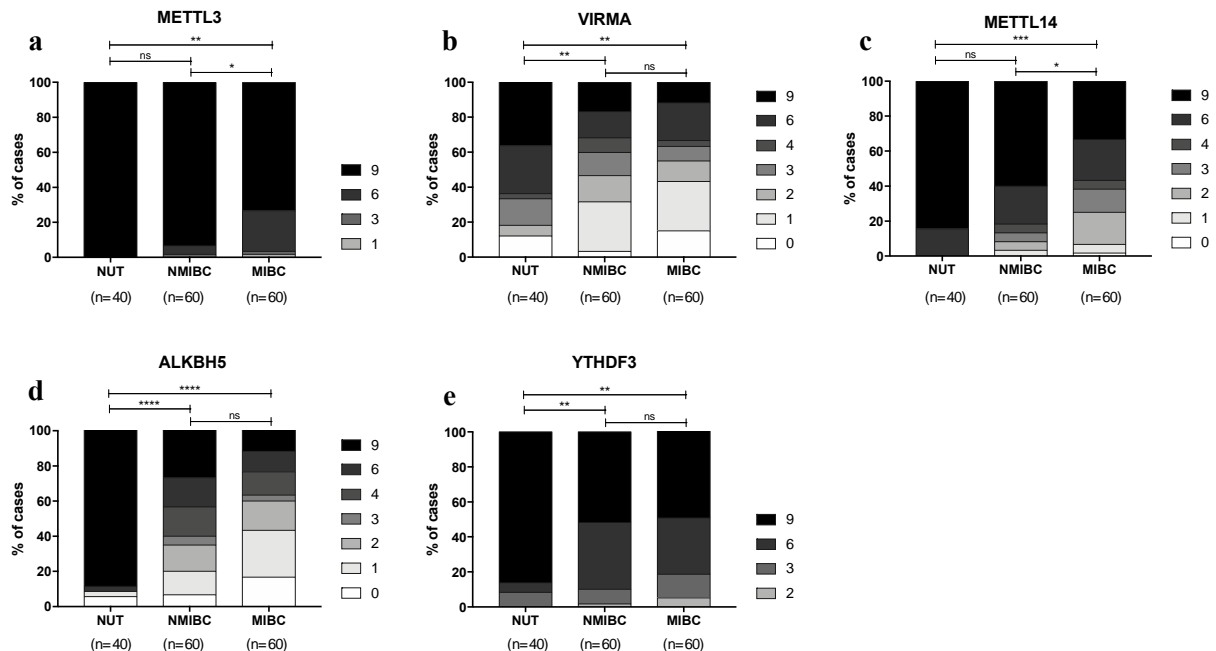


Figure 8. Characterization of METTL3, METTL14, VIRMA, ALKBH5 and YTHDF3 in normal and bladder cancer tissues by immunohistochemistry. **a** METTL3 (NMIBC vs MIBC $p=0.023$; NUT vs NMIBC $p=0.005$), **b** VIRMA (NUT vs NMIBC $p=0.003$; NUT vs MIBC $p=0.006$), **c** METTL14 (NMIBC vs MIBC $p=0.049$; NUT vs MIBC $p=0.003$), **d** ALKBH5 (NUT vs NMIBC $p<0.0001$; NUT vs MIBC $p<0.0001$;) and **e** YTHDF3 (NUT vs NMIBC $p=0.003$; NUT vs MIBC $p=0.006$) immunostaining based on h-score (ranges from 0, +1, +2, +3, +4, +6, +9). Qui-square, * $p<0.05$, ** $p<0.01$, *** $p<0.001$, **** $p<0.0001$, ns- non signification. NUT- normal urothelial tumour, NMIBC- non muscle-invasive bladder cancer, MIBC- muscle-invasive bladder cancer.

The expression of the reader (YTHDF3) and all studied writers positively correlated with m⁶A expression in tumour samples. The same was observed regarding ALKBH5 eraser expression. Interestingly, correlations were also observed between writers and erasers' expression, excepting for WTAP and both the erasers, as well as for VIRMA and FTO. Nonetheless, no correlation was found among the erasers' expression (**Table 5**).

Table 5. Correlation between different regulatory proteins. Spearman's rank correlation coefficient (rho)

	m ⁶ A	METTL3	METTL14	VIRMA	WTAP	FTO	ALKBH5	YTHDF3
m ⁶ A	-	<i>p</i> = 0.001 R= 0.488	<i>p</i> < 0.0001 R= 0.306	<i>p</i> = 0.015 R= 0.223	<i>p</i> = 0.035 R= 0.194	<i>p</i> = 0.081 R=0.162	<i>p</i> = 0.014 R=0.225	<i>p</i> = 0.003 R=0.269
METTL3	-	-	<i>p</i> < 0.0001 R= 0.435	<i>p</i> <0.0001 R= 0.343	<i>p</i> <0.0001 R= 0.415	<i>p</i> = 0.014 R=0.014	<i>p</i> = 0.001 R= 0.294	<i>p</i> <0.0001 R= 0.374
METTL14	-	-	-	<i>p</i> <0.0001 R= 0.373	<i>p</i> = 0.008 R= 0.243	<i>p</i> = 0.066 R=0.169	<i>p</i> <0.0001 R= 0.458	<i>p</i> <0.0001 R= 0.384
VIRMA	-	-	-	-	<i>p</i> = 0.001 R= 0.289	<i>p</i> = 0.309 R=0.094	<i>p</i> <0.0001 R= 0.416	<i>p</i> = 0.011 R= 0.237
WTAP	-	-	-	-	-	<i>p</i> = 0.342 R=0.089	<i>p</i> = 0.131 R= 0.140	<i>p</i> = 0.043 R= 0.192
FTO	-	-	-	-	-	-	<i>p</i> = 0.869 R=-0.015	<i>p</i> = 0.063 R= 0.175
ALKBH5	-	-	-	-	-	-	-	<i>p</i> = 0.097 R= 0.156

We evaluate the association between the expression of the m⁶A regulatory proteins with clinicopathological parameters of the bladder cancer patients.

No significant differences were found for any of the tested proteins expression and patients smoking habits, gender and age of diagnosis. Nonetheless, a significant association was found between METTL3 expression and pathological stage. Indeed, decreased METTL3 expression was displayed by advanced disease (**Figure 9**).

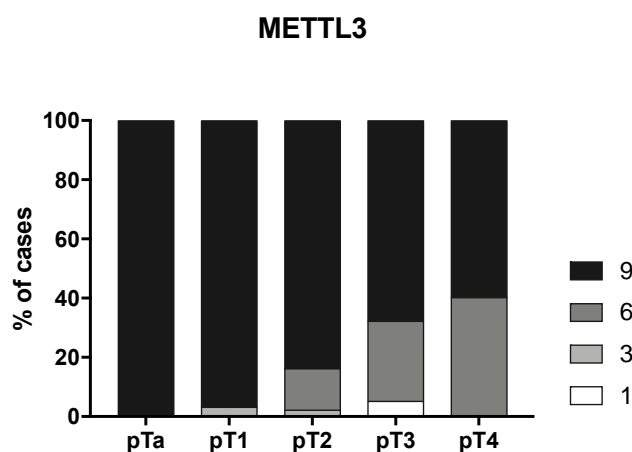


Figure 9. Association between METTL3 protein level and pathological stage. Kruskal-Wallis test (*p*=0.01).

Characterization of METTL3, METTL14, VIRMA, WTAP, ALKBH5, FTO and YTHDF3 protein expression in bladder cell lines

Western blot was performed to evaluate proteins' expression in bladder cell lines.

No differences were apparent for m⁶A regulatory proteins' expression among the tested cell lines, except for METTL14 (**Figure 10a**). Specifically, all BC cell lines presented heterogenous levels of this writer comparing with normal cell line. Among the tumour cells, UMUC3 showed the highest METTL14 expression (**Figure 10b**).

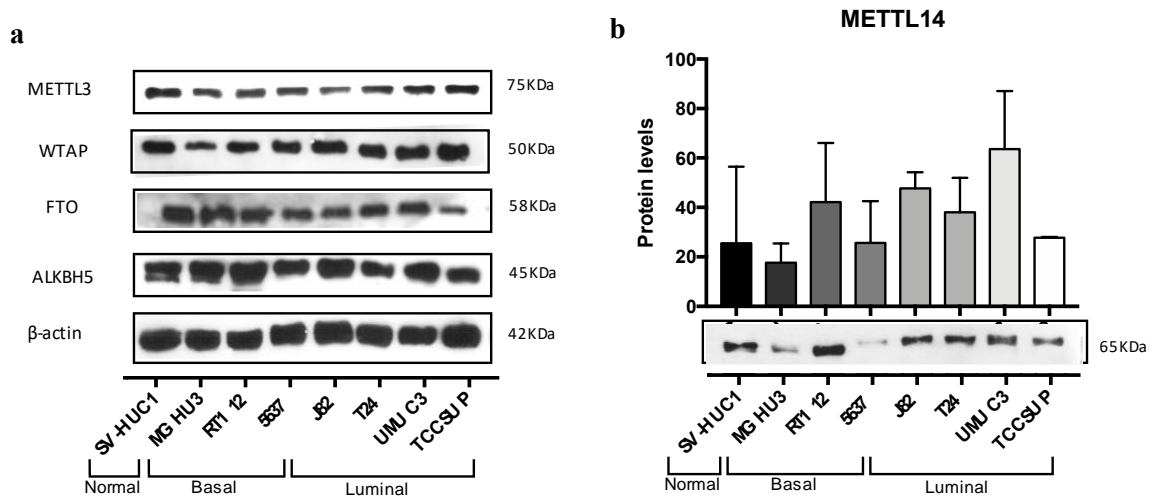


Figure 10. Characterization of regulatory proteins in bladder cancer cell lines a. METTL3, WTAP, FTO and ALKBH5 protein levels in the same cell lines. **b.** The expression of METTL14 protein in 7 bladder cancer cell lines in Western blot. SV-HUC1 cell line was used as control. Kruskal-Wallis test.

Cellular localization of m⁶A and regulatory proteins in cell lines

Immunofluorescence was performed in order to verify cellular localization.

Overall, all writers and erasers were located in the nucleus of all cell lines, whereas the reader was found in the cytoplasm (**Figure 11**), which is in accordance with the observations in primary tumours by IHC.

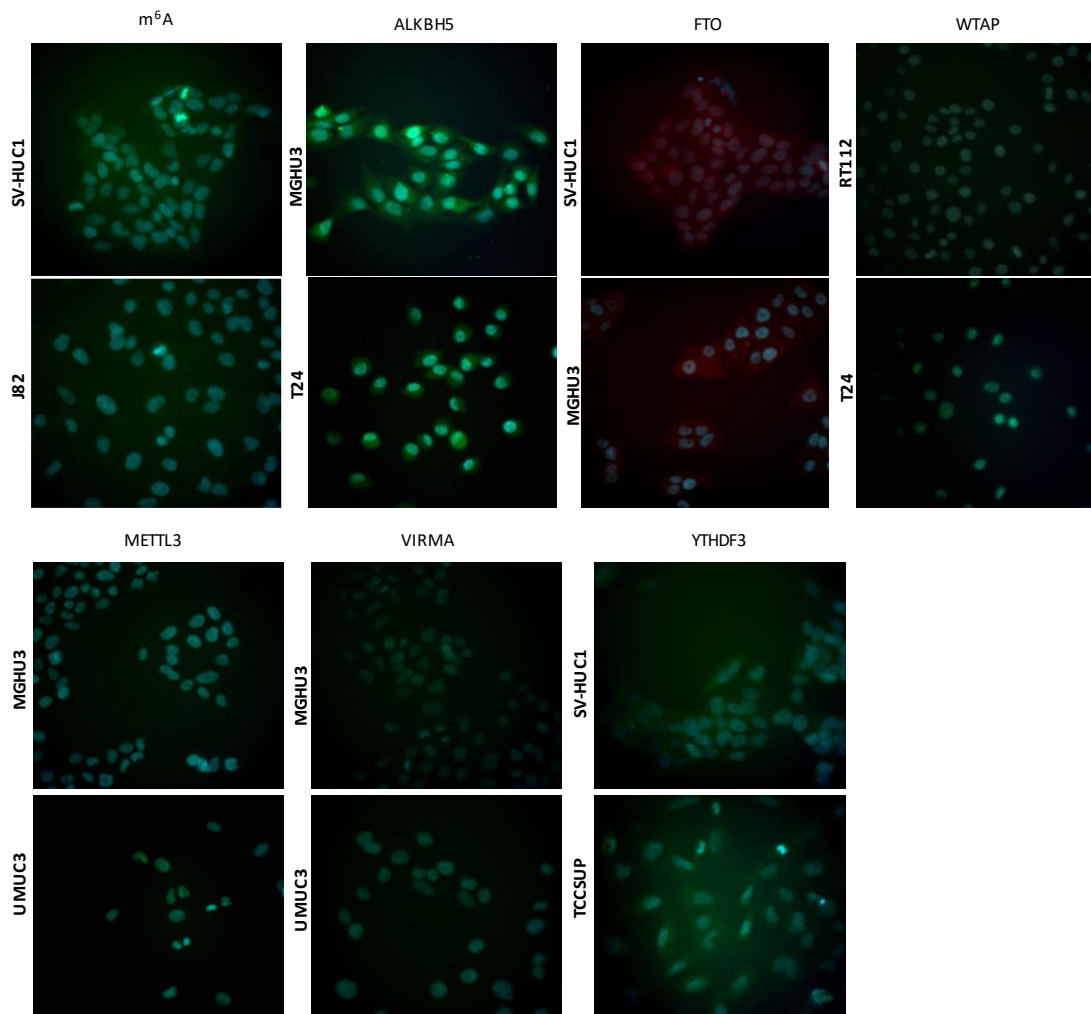


Figure 11. Illustrative images of IF for all tested m⁶A regulatory proteins. Results are compared to negative control. Photograph taken in microscope Olympus IX51 with a digital camera Olympus XM10 (400x amplification).

RNA m⁶A methylation quantification in cell lines

The m⁶A quantification was performed for assess RNA methylation expression levels.

Overall, bladder cancer cells exhibited higher RNA m⁶A methylation percentage comparing with normal cells, although no statistically significant difference was found. Indeed, the highest % was observed in 5637, T24 and UMUC3, with 47%, 29% and 52%, respectively (**Figure 12**).

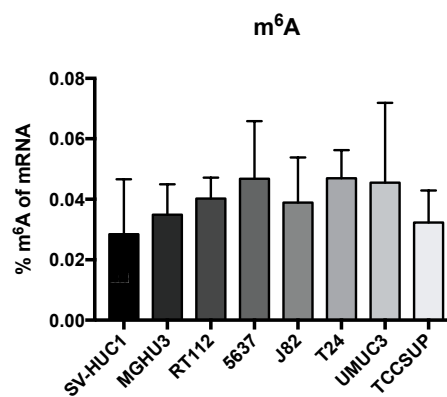


Figure 12. Percentage of m⁶A in mRNA, using the ELISA m⁶A. Kruskal-Wallis test.

CRISPR-Cas9 System in UMUC3

Effective METTL14 knockdown was achieved in UMUC3 cells, confirmed at protein level. A higher efficiency of METTL14 knockdown was accomplished using 1.5 μ L lipofectamine by CRISPR-Cas9 system ($p=0.05$). Specifically, a reduction of about 50% was obtained in UMUC3 cell line (**Figure 13a**), which was paralleled by decreased m⁶A levels in 73% ($p=0.0286$) (**Figure 13b**).

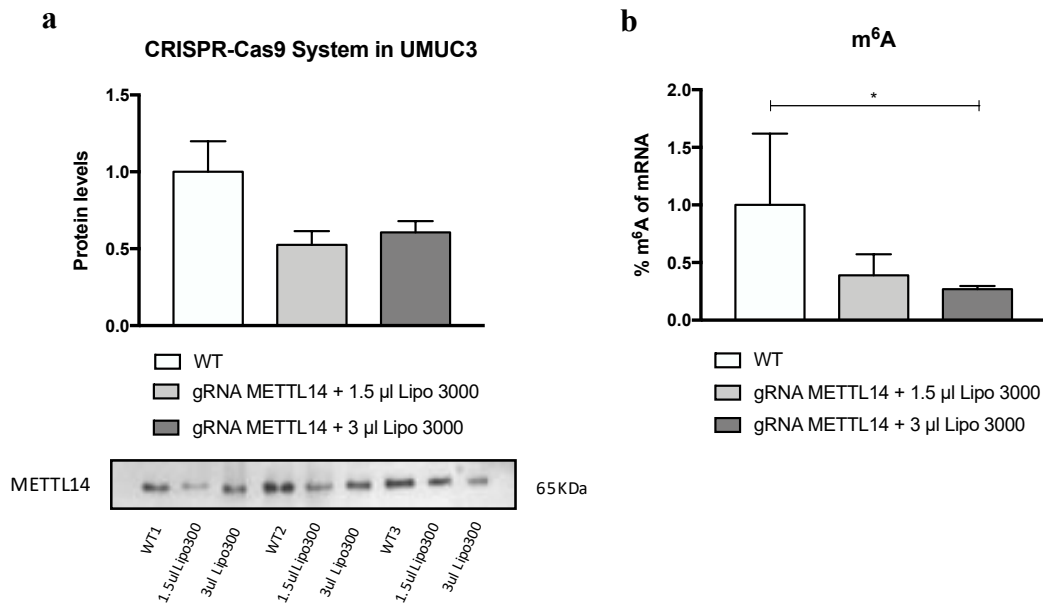


Figure 13. Knockdown of METTL14 on the UMUC3 cell line. **a.** We observed an efficiency in the protein expression of 48% in the condition of 1.5 μ L Lipofectamine 3000 and 40% in the condition of 3 μ L Lipofectamine 3000. Kruskal-Wallis test, $p=0.05$. **b.** Through the colorimetric assay of m⁶A, we found a reduction in the levels of 62% in the condition of 1.5 μ L Lipofectamine 3000 (n.s.) and 73% in the condition of 3 μ L Lipofectamine 3000 ($p=0.0407$). Kruskal-Wallis test: * $p < 0.05$, $p=0.0286$. Abbreviations: WT- Will type.

Phenotypic impact of METTL14 in UMUC3 cell line

Phenotypically, increased cell viability and proliferation was observed in METTL14 knockdown UMUC3 cells at the two different time-points, being more evident at 48 hours ($p<0.001$; $p=0.0033$, respectively) (**Figure 14a/14b**), whereas decreased apoptosis was found at 48 hours (about 3 times, $p=0.0003$) (**Figure 14c**).

Additionally, significantly increased cell invasion was displayed by METTL14 knockdown compared to will-type UMUC3 cells (24 hours, $p=0.0476$) (**Figure 14d**). Notably, METTL14 knockdown significantly increased the migration comparing with will-type UMUC3 cells (48 hours, $p<0.001$) (**Figure 14e**).

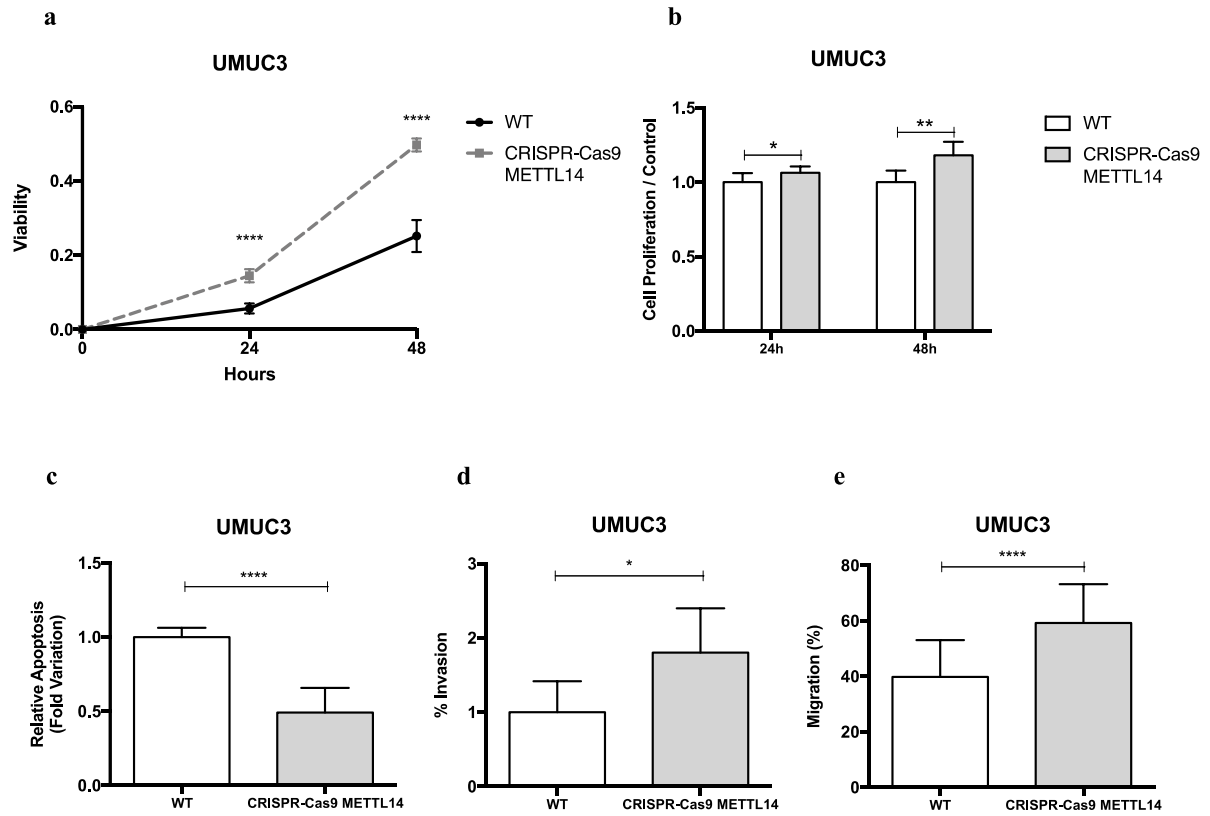


Figure 14. Phenotypic impact METTL14 knockdown in UMUC3 cell line. **a.** in cell viability **b.** in BrdU assay **c.** apoptosis levels after 48 hours (mean \pm SD, n = 3) **d.** cell invasion after 24 hours **e.** cell migration after 48 hours. Mann–Whitney U-test: * $p < 0.05$, ** $p < 0.01$, *** $p < 0.001$ and **** $p < 0.0001$ compared to control (WT: UMUC3). Abbreviations: WT- Will Type.

DISCUSSION

Bladder cancer is one of the most incident urological neoplasms and its treatment remains a major health issue, once survival among patients with advanced disease is rather poor. Hence, the discovery of additional mechanisms underlying disease progression is imperative. m⁶A RNA methylation was firstly reported in 1974 by Ronald Desrosiers, but only recently its function began to be understood (39). Overall, this modification affects numerous aspects of RNA metabolism and plays a critical role in human disease, including cancer (25). Indeed, although m⁶A dysregulation have been reported in several tumours, data on bladder cancer is still limited. Herein, we assessed m⁶A RNA expression deregulation and respective regulatory proteins, also investigating respective role in bladder carcinogenesis.

The selection of more informative m⁶A players was performed by *in silico* analysis of RNA-seq data from muscle-invasive bladder cancer patients available at the TCGA database. METTL3, METTL14, VIRMA, WTAP (components of the m⁶A writer complex), ALKBH5, FTO (components of the m⁶A eraser complex) and YTHDF3 (reader) emerged as the most altered molecules involved in m⁶A regulatory network in bladder cancer. From the seven players, only METTL14 was found to be differentially expressed between tumours and adjacent normal samples.

The protein expression of all the selected “writers”, “erasers” and “reader” was evaluated by IHC analysis in an independent set of bladder tumour and normal tissues. Remarkably, METTL3, METTL14, VIRMA, ALKBH5 and YTHDF3 expression was significantly decreased in bladder cancer compared to normal tissues.

Emerging evidence suggests that, m⁶A regulatory proteins can function both as oncogenes or tumour suppressors. Namely, METTL3, the most described m⁶A writer associated with carcinogenesis was found to be downregulated in endometrial carcinoma and glioblastoma, whereas, upregulation was found in leukaemia, pancreatic, breast and lung cancer (25). Moreover, METTL14 was described to be downregulated in hepatocellular carcinoma acting as a tumour suppressor (40), which is in accordance with our findings.

In our hands, the heterodimeric catalytic core METTL3/METTL14 was significantly reduced in MIBC in comparison with NMIBC, suggesting an association between the methyltransferase complex reduction and more aggressive disease. Also, METTL3/METTL14 expression positively correlated with m⁶A RNA modification, as already reported by others, but for different malignancies (41), reinforcing that writers’ downregulation leads to the complex functionality disruption and consequent reduction in global m⁶A methylation. However, regarding bladder cancer, METTL3 overexpression was also found, but comparing with adjacent normal tissues and not truly normal bladder (3, 23, 42). Nevertheless, these studies used a rather limited number of cases comparing with our patients’ cohort. Furthermore, METTL3 downregulation was found in advanced stages, again in line with the potential bladder cancer prognostic indicator already mentioned. Therefore, our findings add a new layer of epigenetic alterations that might contribute to bladder cancer progression.

Although no studies are available for bladder, VIRMA transcript levels were reported to be significantly higher in liver cancer, which counteract our observations in bladder tumours (43).

Conversely, in line with the results also obtained in glioblastoma patients, in our cohort of bladder cancer patients, ALKBH5 expression was highly heterogeneous in bladder tumours (44).

Remarkably, a correlation was observed between writers and erasers expression in tumours, which might be a mechanism to compensate feedback of descending m⁶A modification, as observed in hepatocellular carcinoma (40).

Indeed, the increase/reduction of m⁶A regulatory proteins, has already been associated with the increase/decrease of m⁶A mark in other tumour models. Particularly, in glioblastoma and hepatocellular

carcinoma, METTL14 downregulation associated with m⁶A levels reduction (40). Indeed, in our set of cell lines, increased m⁶A modification was found in cancer cells compared with normal cells. Interestingly, METTL14 was the only player differential expressed in the same panel of cells, being upregulated in more aggressive tumour cells, particularly in UMUC3 cell line. Herein, METTL14 knockdown accomplished in UMUC3 cells associated with m⁶A levels reduction, suggesting the key role of this protein in complex's function.

In summary, m⁶A-related genes are dysregulated in bladder cancer. Particularly, METTL3/METTL14 methyltransferase complex downregulation is associated with progression of non-invasive bladder cancer to muscle-invasive bladder cancer.

The phenotypic effect of METTL14 knockdown was evaluated in UMUC3 cell line, which resulted in significantly increased cell viability/proliferation, while apoptosis was decreased at 48 hours, contrarily to previous observations in acute myeloid leukaemia cells. Additionally, METTL14 knockdown induced UMUC3 migration and invasion *in vitro*, according to results previously observed by other research team in hepatocellular carcinoma. Hence, our observations support a putative tumour suppressive role in bladder cancer.

Indeed, previous studies, indicate that although METTL14 do not have a catalytic function, it forms a heterodimer with METTL3, required for the complex stabilization and function. Specific interactions between METTL14 methyltransferase domain-MTD14, and METTL3 domain-MTD3, are needed for METTL3 catalytic activity. Hence, METTL3-METTL14 forms a stable methyl capable heterodimer. Wang *et al.* advocate that not only METTL14 structurally supports the METTL3's catalytic cavity, but also has a critical role in substrate RNA recognition (46). In the same line, we found that METTL14 reduction, diminishes the writer complex's activity by reducing m⁶A RNA modification.

CONCLUSION AND FUTURE PRESPECTIVES

In conclusion, since METTL14 knockdown enhances malignant phenotype, one can suggest that METTL14 may have a tumour suppressive role in bladder cancer. Importantly, this is the first comprehensive study on METTL14 function in BC.

In the near future, we intend to ascertain the interaction of the METTL3-METTL14 heterodimer complex, through immunoprecipitation and Site Directed Mutagenesis assay. Furthermore, the downstream pathways regulated by METTL14 will be also investigated.

REFERENCES

1. Bray F, Ferlay J, Soerjomataram I, Siegel RL, Torre LA, Jemal A. Global cancer statistics 2018: GLOBOCAN estimates of incidence and mortality worldwide for 36 cancers in 185 countries. *CA Cancer J Clin.* 2018;68(6):394-424.
2. Monteiro-Reis S, Lobo J, Henrique R, Jeronimo C. Epigenetic Mechanisms Influencing Epithelial to Mesenchymal Transition in Bladder Cancer. *Int J Mol Sci.* 2019;20(2).
3. Jin H, Ying X, Que B, Wang X, Chao Y, Zhang H, et al. N(6)-methyladenosine modification of ITGA6 mRNA promotes the development and progression of bladder cancer. *EBioMedicine.* 2019.
4. Li H-T, Duymich CE, Weisenberger DJ, Liang G. Genetic and Epigenetic Alterations in Bladder Cancer. *Int Neurourol J.* 2016;20(Suppl 2):S84-94.
5. van Kessel K. Personalized Bladder Cancer Management [Ph.D. thesis]: Erasmus University Rotterdam; 2018.
6. Cumberbatch MGK, Jubber I, Black PC, Esperto F, Figueroa JD, Kamat AM, et al. Epidemiology of Bladder Cancer: A Systematic Review and Contemporary Update of Risk Factors in 2018. *European urology.* 2018;74(6):784-95.
7. Berdik C. Unlocking bladder cancer. *Nature.* 2017;551(7679):S34-s5.
8. Mar N, Dayyani F. Management of Urothelial Bladder Cancer in Clinical Practice: Real-World Answers to Difficult Questions. *Journal of Oncology Practice.* 2019;15(8):421-8.
9. Redondo-Gonzalez E, de Castro LN, Moreno-Sierra J, Maestro de las Casas ML, Vera-Gonzalez V, Ferrari DG, et al. Bladder carcinoma data with clinical risk factors and molecular markers: a cluster analysis. *Biomed Res Int.* 2015;2015:168682.
10. Knowles MA, Hurst CD. Molecular biology of bladder cancer: new insights into pathogenesis and clinical diversity. *Nature reviews Cancer.* 2015;15(1):25-41.
11. Sanli O, Dobruch J, Knowles MA, Burger M, Alemozaffar M, Nielsen ME, et al. Bladder cancer. *Nature Reviews Disease Primers.* 2017;3:17022.
12. Comperat E, Varinot J, Moroch J, Eymerit-Morin C, Brimo F. A practical guide to bladder cancer pathology. *Nature reviews Urology.* 2018;15(3):143-54.
13. McConkey DJ, Choi W. Molecular Subtypes of Bladder Cancer. *Current oncology reports.* 2018;20(10):77.
14. Robertson AG, Kim J, Al-Ahmadie H, Bellmunt J, Guo G, Cherniack AD, et al. Comprehensive Molecular Characterization of Muscle-Invasive Bladder Cancer. *Cell.* 2018;174(4):1033.
15. Babjuk M, Bohle A, Burger M, Capoun O, Cohen D, Comperat EM, et al. EAU Guidelines on Non-Muscle-invasive Urothelial Carcinoma of the Bladder: Update 2016. *European urology.* 2017;71(3):447-61.
16. Society AC. Cancer Facts & Figures 2019. 2019.
17. An Introduction to Modern Genetics. By C. H. Waddington. Proceedings of the Royal Entomological Society of London Series A, General Entomology. 1939;14(4-6):82-.
18. Sharma S, Kelly TK, Jones PA. Epigenetics in cancer. *Carcinogenesis.* 2010;31(1):27-36.
19. Kelly AD, Issa JJ. The promise of epigenetic therapy: reprogramming the cancer epigenome. *Current opinion in genetics & development.* 2017;42:68-77.
20. Davalos V, Blanco S, Esteller M. SnapShot: Messenger RNA Modifications. *Cell.* 2018;174(2):498-.e1.
21. Jantsch MF, Quattrone A, O'Connell M, Helm M, Frye M, Macias-Gonzales M, et al. Positioning Europe for the EPITRANSCRIPTOMICS challenge. *RNA Biol.* 2018;15(6):829-31.

22. Coker H, Wei G, Brockdorff N. m6A modification of non-coding RNA and the control of mammalian gene expression. *Biochimica et biophysica acta Gene regulatory mechanisms*. 2019;1862(3):310-8.
23. Cheng M, Sheng L, Gao Q, Xiong Q, Zhang H, Wu M, et al. The m(6)A methyltransferase METTL3 promotes bladder cancer progression via AFF4/NF-kappaB/MYC signaling network. *Oncogene*. 2019.
24. Ianniello Z, Fatica A. N6-Methyladenosine Role in Acute Myeloid Leukaemia. *Int J Mol Sci*. 2018;19(8).
25. Chen XY, Zhang J, Zhu JS. The role of m(6)A RNA methylation in human cancer. *Mol Cancer*. 2019;18(1):103.
26. Meyer KD, Jaffrey SR. Rethinking m(6)A Readers, Writers, and Erasers. *Annu Rev Cell Dev Biol*. 2017;33:319-42.
27. Zhu W, Wang JZ, Xu Z, Cao M, Hu Q, Pan C, et al. Detection of N6methyladenosine modification residues (Review). *Int J Mol Med*. 2019;43(6):2267-78.
28. Dai D, Wang H, Zhu L, Jin H, Wang X. N6-methyladenosine links RNA metabolism to cancer progression. *Cell Death Dis*. 2018;9(2):124.
29. Lan Q, Liu PY, Haase J, Bell JL, Huttelmaier S, Liu T. The Critical Role of RNA m(6)A Methylation in Cancer. *Cancer Res*. 2019;79(7):1285-92.
30. Yue Y, Liu J, Cui X, Cao J, Luo G, Zhang Z, et al. VIRMA mediates preferential m(6)A mRNA methylation in 3'UTR and near stop codon and associates with alternative polyadenylation. *Cell discovery*. 2018;4:10.
31. Zhang X, Wei LH, Wang Y, Xiao Y, Liu J, Zhang W, et al. Structural insights into FTO's catalytic mechanism for the demethylation of multiple RNA substrates. *Proceedings of the National Academy of Sciences of the United States of America*. 2019;116(8):2919-24.
32. Zheng G, Dahl JA, Niu Y, Fedorcsak P, Huang CM, Li CJ, et al. ALKBH5 is a mammalian RNA demethylase that impacts RNA metabolism and mouse fertility. *Molecular cell*. 2013;49(1):18-29.
33. Shi H, Wang X, Lu Z, Zhao BS, Ma H, Hsu PJ, et al. YTHDF3 facilitates translation and decay of N(6)-methyladenosine-modified RNA. *Cell Res*. 2017;27(3):315-28.
34. Cerami E, Gao J, Dogrusoz U, Gross BE, Sumer SO, Aksoy BA, et al. The cBio cancer genomics portal: an open platform for exploring multidimensional cancer genomics data. *Cancer discovery*. 2012;2(5):401-4.
35. Tang Z, Li C, Kang B, Gao G, Li C, Zhang Z. GEPIA: a web server for cancer and normal gene expression profiling and interactive analyses. *Nucleic acids research*. 2017;45(W1):W98-w102.
36. Moch H, Cubilla AL, Humphrey PA, Reuter VE, Ulbright TM. The 2016 WHO Classification of Tumours of the Urinary System and Male Genital Organs-Part A: Renal, Penile, and Testicular Tumours. *Eur Urol*. 2016;70(1):93-105.
37. MB A. *AJCC Cancer Staging Manual Springer*. Internacional Publishing: American Joint Commission on Cancer. 2017.
38. Zuiverloon TCM, de Jong FC, Costello JC, Theodorescu D. Systematic Review: Characteristics and Preclinical Uses of Bladder Cancer Cell Lines. *Bladder cancer (Amsterdam, Netherlands)*. 2018;4(2):169-83.
39. Desrosiers R, Friderici K, Rottman F. Identification of methylated nucleosides in messenger RNA from Novikoff hepatoma cells. *Proceedings of the National Academy of Sciences of the United States of America*. 1974;71(10):3971-5.
40. Ma JZ, Yang F, Zhou CC, Liu F, Yuan JH, Wang F, et al. METTL14 suppresses the metastatic potential of hepatocellular carcinoma by modulating N(6) -methyladenosine-dependent primary MicroRNA processing. *Hepatology (Baltimore, Md)*. 2017;65(2):529-43.

41. Wu L, Wu D, Ning J, Liu W, Zhang D. Changes of N6-methyladenosine modulators promote breast cancer progression. *BMC cancer*. 2019;19(1):326.
42. Han J, Wang J-z, Yang X, Yu H, Zhou R, Lu H-C, et al. METTL3 promote tumor proliferation of bladder cancer by accelerating pri-miR221/222 maturation in m6A-dependent manner. *Molecular Cancer*. 2019;18(1):110.
43. Cheng X, Li M, Rao X, Zhang W, Li X, Wang L, et al. KIAA1429 regulates the migration and invasion of hepatocellular carcinoma by altering m6A modification of ID2 mRNA. *OncoTargets and therapy*. 2019;12:3421-8.
44. Cui Q, Shi H, Ye P, Li L, Qu Q, Sun G, et al. m(6)A RNA Methylation Regulates the Self-Renewal and Tumorigenesis of Glioblastoma Stem Cells. *Cell reports*. 2017;18(11):2622-34.
45. Weng H, Huang H, Wu H, Qin X, Zhao BS, Dong L, et al. METTL14 Inhibits Hematopoietic Stem/Progenitor Differentiation and Promotes Leukemogenesis via mRNA m(6)A Modification. *Cell stem cell*. 2018;22(2):191-205.e9.
46. Wang P, Doxtader KA, Nam Y. Structural Basis for Cooperative Function of Mettl3 and Mettl14 Methyltransferases. *Molecular cell*. 2016;63(2):306-17.